In vitro validation of anticancer drug combinations on colon cancer cell lines SW620 and HCT116

Master of Science in Molecular Medicine

Marianne Greina, May 2018.

NTNU
Norwegian University of
Science and Technology

CONTENT

ACKNOWLEDGMENT

This master thesis is a part of the master program MSc in Molecular Medicine, Faculty of Medicine and Health Science at Norwegian University of Science and Technology (NTNU). The work was performed at the Department of Clinical and Molecular Medicine (IKOM) in the Gastroenterology and Cell system biology research group from August 2017 to Jun 2018.

First, I want to thank my main supervisor, Professor Liv Thommesen for good guidance in this period and for valuable discussion. I also want to thank my co-supervisor PhD student Barbara Niederdorfer for teaching me different techniques, giving me advices during the process and valuable discussion.

ABSTRACT

Combinatory drug treatment, e.g. targeting different proteins in specific signaling pathways tailored to an individual's tumor, is expected to overcome problems related to individual variation in drug efficacy, resistance and side effect. However, our knowledge about beneficial drug combinations is still limited due to the large number of possible drug targets and the tumor diversity. Our research group performed a high throughput screening on multiple cell line to discover synergetic drug combinations on viability. The high throughput screening showed that SW620 cells treated with the inhibitor combination CT+D1 and PI+D1 were synergistic.

The aim of this study was to evaluate and characterize the effect of specific inhibitor combinations initially observed by high throughput screening further and to study the effect of these combinations on another CRC cell line.

We found that the inhibitor combination CT+D1 showed synergetic effect on apoptosis and cell death in the SW620 cell line. In addition, PI+D1 showed synergetic effect on decreased proliferation. These finding were corresponding to the high throughput screening. The inhibitor combination CT+D1 was also synergetic in the HCT116 cell line.

ABBREVIATIONS

CRC	Colorectal cancer
TP53	Tumor protein p53
APC	Adenomatous polyposis coli
PI3K	Phosphatidylinositol-4, 5-bisphosphate -3 kinase
PIK3CA	Phosphatidylinositol-4, 5-bisphosphate 3-kinase catalytic subunit alpha
RAS	The Rat Sarcoma
KRAS	Kirsten Rat Sarcoma
RTK	Receptor tyrosine kinase
EGFR	Epidermal growth factor receptor
PIP2	Phosphatidylinositol (4,5)-bisphosphate
PIP3	Phosphatidylinositol (3,4,5)-trisphosphate
PTEN	Phosphatase and tensin homolog
PDK1	3-phosphoinositide-dependent protein kinase 1
AKT	Protein Kinase B
mTORC1	Mammalian target of rapamycin complex 1
GRB2	Growth factor receptor-bound protein 2
SOS	Son of sevenless
GDP	Guanosine diphosphate
GTP	Guanosine triphosphate
Raf	Rapidly accelerated fibrosarcoma
MEK	Mitogen-activated protein kinase kinase
ERK	Extracellular signal-regulated kinase
RSK	Ribosomal S6 kinase
S6K	Ribosomal protein S6 kinase
GSK3	Glycogen synthase kinase 3
MAD1	Mitotic arrest deficient protein 1
MAX	MYC associated factor X
RB	Retinoblastoma
TNF	Tumor necrosis factor
FAS	Apoptosis stimulating fragment
FADD	Fas-associated protein with death domain
DISC	Death-inducing signaling complex
BAD	BCL-2-associated agonist of cell death
HSA	Highest single agent

1. INTRODUCTION

The development of personalized medicine is driven by the rapid improvement of technology that provides high throughput data from different "omics" experiments (genomic, transcriptomic, proteomic and metabolomics). It is expected that this data will give us a better understanding about the regulation of transcription and translation, and the cause of diseases and by this contribute to better diagnostics, prognosis and treatment of patients (Collins, 2015).

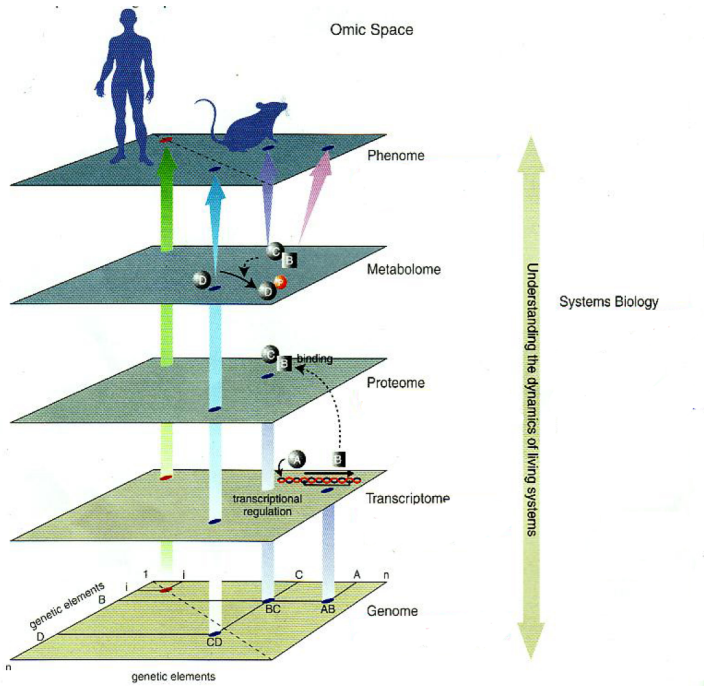

Figure 1: The different omics levels. Modified from (RIKEN, 2006).

Knowledge of intracellular signaling pathways has led to the development of target-specific drug treatment, e.g. anti-EGFP therapy. However, there are still challenges related to the design of effective and specific drugs and to the development of drug resistance. Combinatory drug treatment, e.g. targeting different proteins in specific signaling pathways, tailored to an individual's tumor is expected to overcome problems related to individual variation in drug efficacy, resistance and side effect (Al-Lazikani, 2012; Collins, 2015). However, our knowledge about beneficial drug combinations is still limited due to the large number of possible drug targets and the tumor diversity.

High throughput screening is a well-known technique that uses laboratory robotics in biological scientific research. This method is automatable, easy, fast, cheap and non-invasive that can perform set-ups with thousands of samples. With this automatable approach, scientists can

easily use large datasets from these high throughput screenings to answer complex biological questions. This approach reduces cost and time consuming wet lab experiments and can be the answer to discover synergetic drug combinations (Szymański, 2012).

1.1 COLORECTAL CANCER

Colorectal cancer (CRC) is one the most frequently diagnosed cancers worldwide. Among men, CRC ranked third in prevalence after lung and prostate cancers. Among women, CRC ranked second in prevalence after breast cancer (Navarro, 2017). CRC in 2012 accounted for nearly 1.4 million diagnosed cases and almost 700 000 deaths worldwide (Ferlay, 2015). CRC incidence and mortality show wide geographical variations across the world. The highest estimated CRC-related mortality rates in both sexes were found in Central and Eastern Europe, and the lowest were found in Western Africa (Ferlay, 2015). CRC is the second most common form of cancer in Norway (Guldvog, 2017). In 2015, there were 1152 death related to CRC reported in Norway, of which 547 were men and 605 woman (Larsen, 2016).

A Norwegian nationwide endoscopy screening program for CRC will be established during 2019 (Guldvog, 2017), aiming to reduce mortality among CRC patients. This screening program will probably reduce disease-specific mortality by 27% or more and the incidence of intestinal cancer will then be reduced by 22% or more (Guldvog, 2017).

The primary symptoms of CRC are persistent rectal bleeding and changes in bowel habits. Later symptoms include anemia and intestinal obstruction. However, the symptoms in CRC are vague which often results in detection of the disease at the late state. The main treatment of CRC is surgery, but this treatment is not always effective due to metastases. Chemotherapy and radiotherapy is utilized as a complementary treatment to surgery, however side effects and drug resistance due to diversity in individual tumors (heterogeneity) still occurs (Collins, 2015). The medical treatment for CRC is limited and the need for better therapies is crucial (Collins, 2015; Marsh, 2007).

CRC is a disease originating from the epithelial cells lining the colon or rectum of the gastrointestinal tract. The most common type is adenocarcinoma, which occurs in approximately 95% of the cases. Development of colon carcinogenesis involves progression from hyper-proliferative mucosa, to transformation into non-invasive lesions and subsequent tumor cells with invasive and metastatic capabilities (Marsh, 2007).

On the molecular level, cancer results from the presence of multiple mutations. These mutations often occur in proteins controlling cell growth, proliferation and survival (Hanahan, 2011). In the article by Hanahan and Weinberg, six main hallmarks required for cancer development are described (Figure 2.) Cancer progression may start with a single mutation in a growth factors signaling pathway. Other mutations can cause evading of growth suppression and loss of function of tumor suppressor proteins and uncontrolled cell division leading to higher levels of mutation introducing immortality, induction of angiogenesis and activation of invasion and metastasis (Hanahan, 2011).

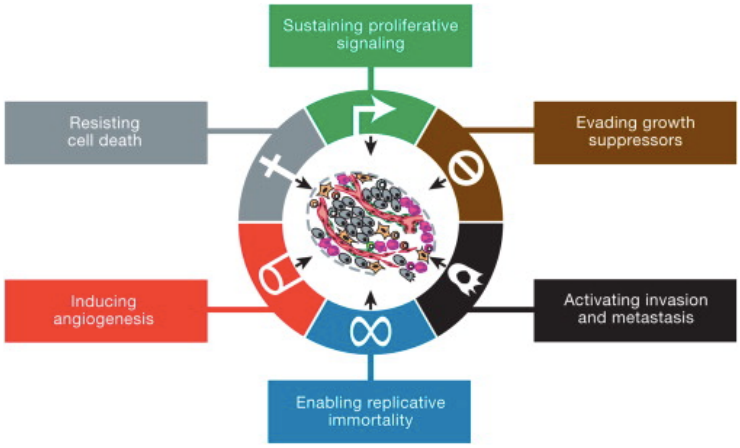

Figure 2: The six main hallmarks for cancer development (Hanahan, 2011).

The driver mutations in the development of CRC involves the activation of oncogenes and inactivation of tumor suppressor genes. The tumor protein p53 (TP53) gene encodes the tumor suppressor transcription factor p53 that plays a role in regulating cellular responses to DNA damage. p53 activation leads to cell cycle arrest and DNA repair upon damage and initiates apoptosis when DNA damage is irreparable. Upon mutation, more mutations will be accumulated in the cell and eventually lead to cancer development (Nejad, 2012). p53 mutation occurs in approximately 40%-50% of CRC (Takayama, 2006). Different types of p53 mutations play a pivotal role in determining the biologic behavior of CRC, such as invasive depth, metastatic site and even the prognosis of patients (Xiao-Lan, 2015).

Adenomatous polyposis coli (APC) is a tumor suppressor gene. Mutations in the APC gene occur often in CRC, and are likely to be the initiating events in tumorigenesis (Schell, 2016). The canonical tumor suppressor function of APC is to prevent the accumulation of the oncogene β-catenin in the absence of Wnt signaling. Mutations in the APC gene results in β-catenin

accumulation and translocation into the nucleus where transcription of proto-oncogenes is activated. The tumorigenic consequences of unregulated β-catenin activity may be related to the direct stimulation of cellular growth and proliferation (Kwong, 2009; Schell, 2016).

Phosphatidylinositol-4, 5-bisphosphate -3 kinase (PI3K) participates in the PI3K/AKT/mTOR signaling pathway. The oncogene phosphatidylinositol-4, 5-bisphosphate 3-kinase catalytic subunit alpha (PIK3CA) is described to be mutated in various cancer (Samuels, 2010), and has been reported in 10-20% of CRC (Ogino, 2014). The presence of a mutated PIK3CA is associated with constitutive-activation of the PI3K/AKT/mTOR signaling pathway and further activation of cell proliferation and survival (Cathomas, 2014).

The Rat Sarcoma (RAS) proto-oncogene encodes for proteins (KRAS, HRAS and NRAS) which belong to the small GTPase superfamily. RAS proteins recruits and activate downstream effectors, such as those of the AKT and ERK pathways. The presence of RAS mutations is associated with cell proliferation and survival (Lievre, 2006). Approximately 35-45% of CRC tumors are known to involve mutated Kirsten Rat Sarcoma (*KRAS)* oncogene (Tan, 2012).

1.2 CELLULAR SIGNALING

Growth factors and hormones mediate communication between cells and acts via their specific receptors. These receptors are often located at the plasma membrane where binding of agonists result in activation of intracellular signaling pathways. The signaling cascades involve protein phosphorylation/dephosphorylation, transcriptional activation and altered cellular characteristics (Alberts, 2009).

1.2.1 RECEPTOR TYROSIN KINASE

Receptor tyrosine kinase (RTK) signaling pathways regulates cell proliferation, differentiation and cell survival (Lemmon, 2010). The RTKs have an extracellular domain for ligand binding, a membrane spanning segment and a cytoplasmic domain. To activate the intracellular tyrosine kinase domain in RTK, two RTKs are dimerize upon ligand binging and phosphorylated. The phosphorylated tyrosines are the docking site for intracellular adaptor proteins and mediates the response of growth factor (Alberts, 2009). A constitutive activation of RTK due to a mutation of the receptor may influence proliferation or evasion of apoptosis, and may lead to uncontrolled growth and tumor formation (Hanahan, 2011).

There are two types of commercial drugs available that targets RTKs. One type involves inhibitors targeting the ATP binding site in the intracellular tyrosine kinase domain (Shawver, 2002), the other type is based on monoclonal antibodies which interfere with RTK activation by preventing receptor dimerization (Reichert, 2007). Imatinib was the first RTK inhibitor on the marked (Shawver, 2002). This inhibitor targeted the ATP binding site in the intracellular tyrosine kinase domain, hampering phosphorylation and activation. However, this compound lacks specificity because of the ATP binding site is conserved among many kinases causing inhibition of off-target RTKs. Another problem was patients developed drug resistance (Shawver, 2002).

The epidermal growth factor receptor (EGFR) belongs to the ErbB-family. The drugs Cetuximab and Panitumumab are monoclonal antibodies targeting the EGFR, preventing activation of multiple downstream signal transduction cascades (Zhao, 2017). Among the major downstream pathways activated by EGFR are the RAS-MAPK-ERK and PI3K-AKT pathways. Mutations in proteins involved in these pathways, such as KRAS and PIK3CA mutations, is reputed to constitutive activation of these downstream pathways and results in EGFR drug resistance (Zhao, 2017). Resistance to anti-EGFR therapy is often present in CRC. The next strategy is therefore to target protein downstream of the RKTs (Logue, 2012).

1.2.2 PI3K-mTOR SIGNALING PATHWAY

The activation of RTK recruits PI3K to the receptor and leads to phosphorylation of the PI3K protein. The phosphatidylinositol (4,5)-bisphosphate (PIP2) and phosphatidylinositol (3,4,5)-trisphosphate (PIP3) are located on the cytosolic side of the plasma membrane and constitute as an on-off switch (Figure 3). PIP2 prevents further signaling in the pathway while PIP3 activates the downstream cascade. There are two proteins controlling this on-off switch, phosphatase and tensin homolog (PTEN) and PI3K. Active PI3K phosphorylates PIP2 into PIP3, resulting in activation of the signaling pathway. PTEN removes phosphate from PIP3 and by this acting as negative regulator. PIP3 recruits both 3-phosphoinositide-dependent kinase 1 (PDK1) and protein kinase B (AKT) to the cell membrane where they interact with each other. PDK1 phosphorylates AKT Thr308, which leads to a partial activated kinase. To become fully activated, AKT also need to be phosphorylated on Ser473 by the mammalian target of rapamycin complex 1 (mTORC1) complex (Danielsen, 2015; Mendoza, 2011). In CRC a constitutive PI3K-mTOR signaling is driven by mutations in EGFR and PI3KCA (Hong, 2016).

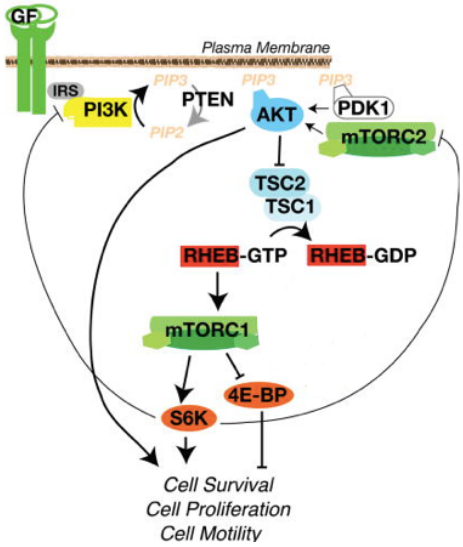

Figure 3: P13K-mTOR pathway. Modified from (Mendoza, 2011).

1.2.3 RAS-MAPK-ERK SIGNALING PATHWAY

Activation of RTK recruits growth factor receptor-bound protein 2 (GRB2) that binds to the phosphorylated tyrosine residues of the receptor (Figure 6). The GRB2 protein forms a complex with son of sevenless (SOS) which results in the activation of SOS proteins. Active SOS recruits the RAS protein and exchange guanosine diphosphate (GDP) to guanosine triphosphate (GTP). RAS bound to GTP phosphorylates rapidly accelerated fibrosarcoma (Raf), which is the initial step in the kinase-phosphatase cascade (Figure 4). Eventually, extracellular signal-regulated kinase (ERK) and ribosomal S6 kinase (RSK) promote cell survival, cell proliferations and cell motility (Fang, 2005; Mendoza, 2011). In CRC a constitutive Ras-MAPK-ERK signaling is driven by mutations in EGFR, KRAS and B-RAF (Hong, 2016).

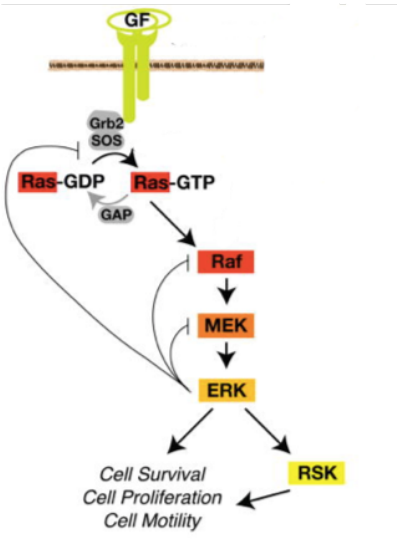

Figure 4: The Ras-MAPK-ERK pathway. Figure modified from (Mendoza, 2011).

RSK, AKT, and ribosomal protein S6 kinase (S6K) may act on the same substrate, e.g. glycogen synthase kinase 3 (GSK3) and BCL-2-associated agonist of cell death (BAD) as shown in figure 7 (Mendoza, 2011). These kinases (RSK, AKT and S6K) inactivates the GSK3 α/β kinases, by phosphorylation on Ser21/Ser9, that leads to GSK3-mediated inhibition of cell survival, proliferation and motility (Mendoza, 2011). BAD induces apoptosis by neutralizing the pro-survival BCL2 protein family. RSK phosphorylate BAD at Ser112, while AKT and S6K phosphorylate BAD on Ser136. The 14-3-3 proteins bind p-BAD which promotes cell survival by sequestering BAD in the cytosol, away from pro-survival BCL2 family members (Mendoza, 2011; She, 2005).

1.2.4 DRUG TARGETING

The knowledge about crosstalk between different signaling pathways has revealed the complexity of intracellular signaling pathway. Crosstalk and pathway convergence could theoretically contribute to low drug efficiency to drugs targeting only one pathway (Mendoza, 2011). A cross talk between P13K-AKT and MAPK-ERK signaling have been observed in the breast cancer cell line MCF7 (Carracedo, 2008). These cells exhibited phosphorylation and high activity of ERK, EGFR and RAS. Interestingly, treatment with MEK inhibitors increased AKT activity and induced cell growth, not cell death as expected. When cells were treated with the combination of MEK and P13K inhibitors, Carracedo et al. observed enhanced cell death compared to P13K or MEK inhibitors alone (Carracedo, 2008).

It is well known that combinatory drug treatment, i.e. targeting different proteins in specific signaling pathways, is expected to give a better drug efficacy, fewer side effects and probably reduce the drug resistance (Al-Lazikani, 2012; Collins, 2015). However, our knowledge of beneficial drug combinations is still limited due to large number of possible drug targets.

Our research group performed a high throughput screening on multiple cell lines with the purpose to see drug effect on viability after 48h. The aim was to discover synergistic effect; inhibitors (A+B) have an increased effect compare to (A) and (B) alone. Synergy was calculated by the highest single agent approach (HSA). HSA is considered a well-used approach to assess the combined effects of drugs. HSA excess reflects if the effect of a drug combination (A+B) is greater than the effects produced by its individual components (A,B) (Foucquier, 2015).

$$HSA\ excess = E(A,B) - E(A+B)$$

The chosen cut-off value for synergetic effect was -0.12.

The dose response curves form the CRC cell line SW620 treated with the inhibitors BI-D1870 (D1), PI-103 (PI) and CT99021 (CT) is shown in Figure 5.

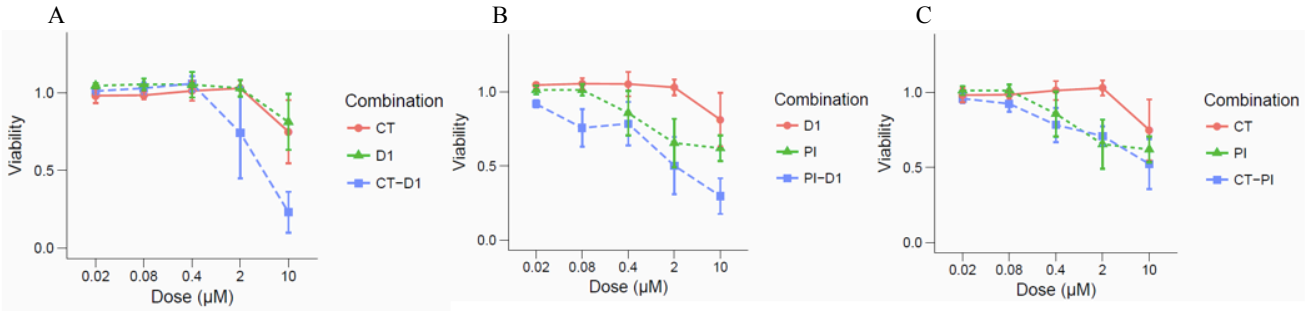

Figure 5: Viability of SW620 cells treated with different inhibitor for 48h. (CellTiter-Glo) (Flobak Å, Niederdorfer B, manuscript in progress) (PI:PI-103, CT:CT99021, D1:BI-D1870).

These results show that SW620 cells treated with the inhibitor combination CT+D1 and PI+D1 are synergistic. These various drugs target specific proteins in different pathways; described above under paragraphs 1.2.2 P13K-mTOR signaling pathway and 1.2.3 The Ras-MAPK-ERK pathway. D1 is targeting p90RSK, PI is targeting PI3K and CT is targeting GSK3 (Figure 6).

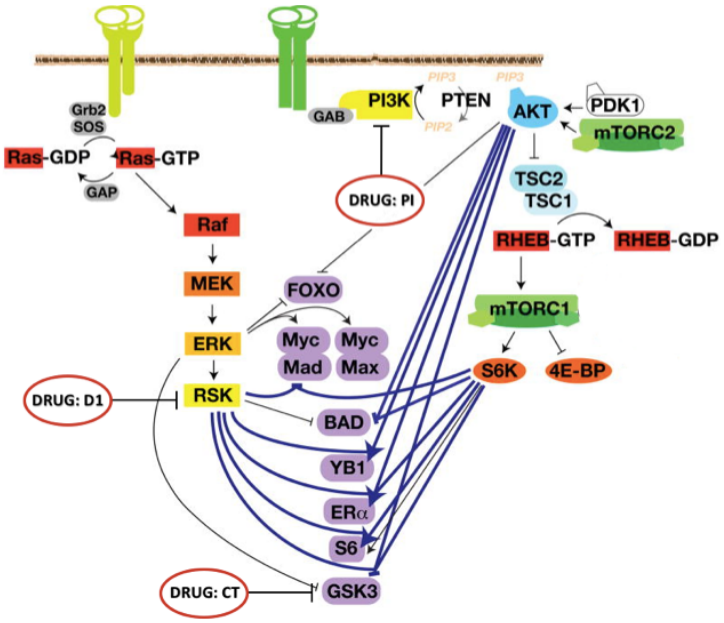

Figure 6: The target specific inhibitors used in this study. Modified from (Mendoza, 2011).

1.3 TRANSCRIPTION FACTOR

Intracellular signaling often leads to the activation of transcription factor. A transcription factor is a protein that controls the rate of transcription of genetic information from DNA to messenger RNA, by binding to a specific DNA sequence.

1.3.1 MYC

The transcription factor MYC ability to bind to the DNA and activate transcription is depending on the balance between the MYC/MAX/MAD network (Figure 7). The AKT/mTOR pathway affects this network. S6K1 phosphorylates and inhibits the tumor-suppressor function of mitotic arrest deficient protein 1 (MAD1) (Cascón, 2012). Functional MAD1 competes with MYC associated factor X (MAX) for the binding to MYC. Inhibition of MAD1 lead to MYC/MAX binding and positively regulate growth and survival transcriptional programs (Cascón, 2012; Mendoza, 2011).

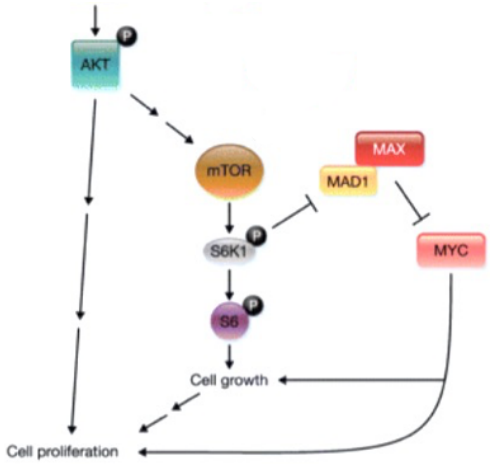

Figure 7: The AKT/mTOR pathway effect on MYC transcription factor. Modified from (Cascón, 2012).

The MYC is also activated by the ERK-pathway. RSK degenerate MAD1 trough phosphorylation and leads to the binding between MYC/MAX. In both pathways (AKT-mTOR and ERK), functional MAD1 leads to the binding of MYC/MAD1. This results in suppressed MYC´s transcription activity and reduce cell growth and cell proliferation (Mendoza, 2011).

Many human tumors display elevated levels of MYC. Overexpression of MYC promotes oncogenic transformation and tumorigenesis by activation the transcription of target genes that drive cell proliferation and stimulate angiogenesis (Cascón, 2012).

1.3.2 E2F

The transcription factor E2F plays a crucial role in regulating cell proliferation since this protein controls the expression of many genes that are required for cell cycle progression. The retinoblastoma tumor suppressor protein (RB) binds to the E2F transcription factor preventing it from interacting with transcription machinery. In the absence of RB, E2F mediates the activation of E2F target genes that promotes proliferation, at the G1/S transition and S-phase (Chaussepied, 2004).

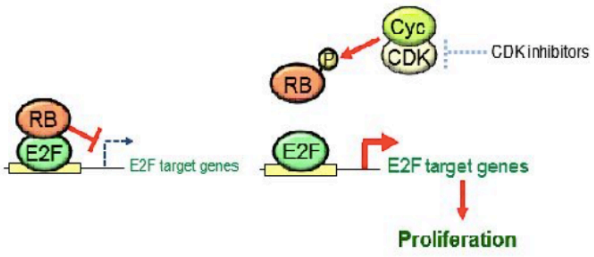

Figure 8: The regulatory mechanism of the transcription factor E2F by the RB pathway (Ozono, 2013).

Disruption of the RB pathway and subsequent activation of E2F is regarded to be an essential event for tumorigenesis. Mutation of the RB gene is observed in about 30% of cancers (Ozono, 2013).

1.4 APOPTOSIS

Apoptosis is a vital process in multicellular organisms (Elmore, 2007). Apoptosis is involved in normal cell turnover, crucial for proper development of fetus and differentiation of the immune cells. Deregulation of apoptosis is involved in many pathophysiological conditions such as neurodegenerative diseases, ischemic damage, autoimmune disorders and plays a crucial role in many types of cancer (Elmore, 2007). Apoptotic cells are characterized by nuclear condensation, cell shrinkage, membrane blebbing and DNA fragmentation (Elmore, 2007).

Caspases, a family of cysteine proteases, are crucial in the regulation of apoptosis (Elmore, 2007). Initiator caspases (including caspase-2,-8,-9,-10,-11 and -12) are tightly coupled to pro-apoptotic signals. Once activated, these caspases cleave and activate downstream effector caspases (including caspase-3,-6 and-7), which in turn execute apoptosis (Elmore, 2007; Hotchkiss, 2009).

Apoptotic signaling is divided into either the intrinsic or the extrinsic pathways (Figure 9) The intrinsic pathway of apoptosis is activated by receptor-independent stimuli such as radiation, free radicals, viral infections or from intracellular signal proteins (Elmore, 2007).

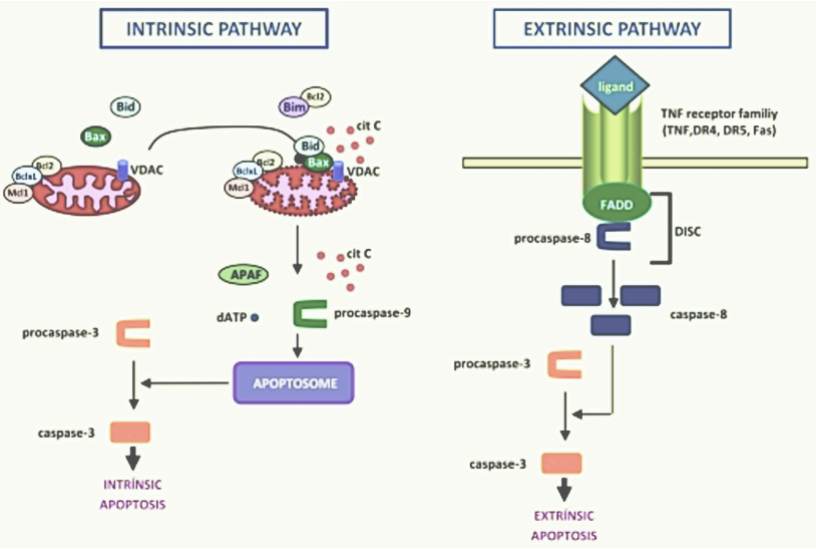

Figure 9: Intrinsic and extrinsic pathway in apoptosis. Modified from (Gómez-Sintes, 2011)

The intrinsic pathway of apoptosis involves changes in the permeability of the inner mitochondrial membrane. The consequences of this change are loss of the mitochondrial trans-membrane potential and the release of pro-apoptotic proteins, e.g. cytochrome C. Cytochrome C interact with caspase 9, and this active complex forms the apoptosome. This leads to further activation of caspase 3, that results nuclear fragmentation (Jourdain, 2009). In cancer cells, like CRC, constitutively activated signaling pathways like the PI3K-AKT-mTOR and/or RAS-MAPK-ERK pathways suppress apoptosis (Hotchkiss, 2009).

The extrinsic pathway is activated through binding of a ligand to its specific receptor on the cell surface (Figure 9). It is also referred to the death-receptor pathway, and the most described ligand is apoptosis stimulating fragment (FAS) ligand (Hotchkiss, 2009). FAS ligand, with it complementary death receptor, are both a member of the tumor necrosis factor (TNF) family (Hotchkiss, 2009). The activation by FAS ligand leads to a trimerization of the receptor, which recruits the adopter protein Fas-associated protein with death domain (FADD) to the receptor intracellular domain. Together with caspase 8, the activated receptor and FADD forms a death-inducing signaling complex (DISC) (Jin, 2005). DISC, in the end, activates effector caspases 3, that results nuclear fragmentation (Jin, 2005).

1.5 AIM OF THE STUDY

Combinatory drug treatment, e.g. targeting different proteins in specific signaling pathways, tailored to an individual's tumor is expected to overcome problems related to individual variation in drug efficacy, resistance and side effect. Our research group performed a high-throughput screening to discover synergetic drug combinations.

The aim of this study was:

- To evaluate and characterize the effect of specific inhibitor combinations initially observed by high throughput screening further and to study the effect of these combinations on another CRC cell line. (Confirm/disprove synergic)

This was performed by assessing changes in morphology and by measuring protein expression, cell death, confluency and activation of transcription factors. Cell death was characterized by metabolic and apoptosis assays.

2. MATERIAL AND METHODS

2.1 CELL LINES AND REAGENTS

The human CRC SW620 (human colorectal adenocarcinoma) and HCT116 (human colorectal carcinoma) cell lines were utilized (ATTC, Rockville, Maryland). The cells were cultivated in RPMI Medium 1640 (Gibco, Invitrogen) supplemented with 100 ug/ml penicillin-Streptomycin (Gibco, Invitrogen) and 10 % fecal calf serum (FCS) (Gibco, Invitrogen) at 37°C with 5% pCO_2.

The chemical inhibitors used were: CT99021 (Sigma) targeting GSK3, BI-D1870 (Selleckchem) targeting p90RSK and PI-103 (Selleckchem) targeting PI3K. The inhibitors were dissolved in dimethylsulfoxide (DMSO) with a stock concentration of 20mM and stored at -80°C. In all the performed experiments, the highest drug concentration did not exceed 0,1% DMSO.

2.2 WESTERN BLOT

The cells were seeded out in six well plates with 400 000 cells/well (HCT116) and 800 000 cells/well (SW620) in 2ml/well and cultivated for 24 hours. Then the cells were treated with inhibitors at concentration 0.4µM, 2µM and 10µM for 24 hours. The cells were detached from the plates using trypsin, followed by addition of phosphate buffered saline (PBS) supplemented with 10% FCS, respectively. The cells were collected and centrifuged at 1500 rpm at 4°C for 8 minutes. The cell pellet was resuspended in 1 ml cold PBS and centrifuged again. The supernatant was discarded, and the pellet was snap frozen in liquid N_2. For immunoblot detection of phosphorylated protein and total proteins, Tris-Buffer was utilized. Approximately twice the amount of the cell pellet size of Tris-buffer I and II (Appendix 1) was added to the cell pellet. The cells were then incubated for 1 hour on a shaker at 4°C, and centrifuged again at 16 000 rpm at 4°C for 15 minutes before the lysate was transferred to new tubes and stored at -80°C.

1µl of the protein lysate was diluted in 1 ml of dH_20 to determine the protein concentration. 250µl of Bio-Rad protein assay Dye Reagent (Bio-Rad, 500-0006) was added and the absorbance of the solution was assessed at λ=595 nm (ThermoSpectronic Genesys 20).

The amount of protein loaded per well on the gel was 40 µg. The samples were run and prepared as follows. The protein samples were mixed with 5 µl NuPage LDS Sample Buffer (4x, Invitrogen, #NP0008), 1 µl DL-Dithiothreitol solution (DTT, 1M, Sigma, #646563) and Tris buffer (10mM). The samples were denatured by being placed in a heating block (70°C) for 7 minutes. The samples and the marker ((4.5µl SeeBlue Plus2 pre-stained protein standard (Invitrogen, LC5925) + 1.5µl MagicMark XP western protein standard (Invitrogen, LC5602)) were separated by size using NuPAGE gel (Novex) with 1x MOPS SDS running Buffer (NuPAGE, NP0001). The gel was run at 200 V for 50 minutes.

The immobilon Transfer Millipore Membrane – PVDF with pore size 0.45 µm was activated by placing it for 10 sec in methanol, water and 1x Transfer Buffer (NuPAGE, NP0006-1) supplemented with 10% methanol. The proteins were blotted to the membrane using the Xcell II Blot Module (Invitrogen) and 1x Transfer Buffer supplemented with 10 % methanol. The proteins were blotted for 1 hour at 30 V. The membrane was dried for 10 minutes at 60 °C, reactivated by methanol, water and Tris-buffered saline with Tween20 (TBST), respectively, and blocked in 5% blocking detergent bovine serum albumin (BSA, Sigma). Furthermore, the membrane was incubated with the primary antibody diluted in 1 % BSA, washed in TBST prior to secondary antibody incubation and development of the membrane.

The substrate ”SuperSignal West Femto Maximum Sensitivity Substrate” (Pierce, Thermo Scientific, 34095) was used to detect HRP-probed antibodies. The incubation time varied from 10 sec to 2 min and 30 sec, depending on primary antibody used. Chemiluminescent was detected using Odyssey FC (LI-COR). The incubation time of emission light varied from 30 sec to 2 min. The images were analyzed using Image Studio. The relative protein expression was normalized to a loading control. The changes in signal of each band was determined by comparing the normalized signal in treated versus untreated sample.

Table 1: List of antibodies.

Antibodies	Molecular weight	Company	Dilution
Phospho-AKT (Ser473) Rabbit mAb	60 kDa	Cell Signaling #4060S	1:1000
Phospho-GSK-3α/β (Ser21/9) Rabbit pAb	46/51 kDa	Cell Signaling #9331S	1:1000
Phospho-BAD (Ser112) Rabbit pAb	23 kDa	Cell Signaling #9291S	1:1000
Total AKT Mouse mAb	60 kDa	Cell Signaling #2920S	1:1000
Total GSK-3α/β Mouse mAb	46/51 kDa	Santa Cruz #Sc:7291	1:1000
Total BAD Rabbit pAb	23 kDa	Cell Signaling #9292S	1:1000
PCNA (PC10) Mouse mAb	36 kDa	Santa Cruz #56	1:5000
Swine Anti-Rabbit pAb HRP	-	Dako #P0399	1:5000
Goat Anti-Mouse pAb HRP	-	Dako #P0447	1:5000

2.3 CELLTOX-GREEN ASSAY

The CellTox-Green Cytotoxicity Assay (Promega, #256687) is based on the changes in membrane integrity the occur as a result of cell death. This assay uses a proprietary asymmetric cyanine dye that is excluded from viable cells. When the dye binds DNA in dead cells, the dyes fluorescent properties are substantially enhanced (Figure 10). Viable cells produce no appreciable increases in fluorescence, so the fluorescent signal is proportional to cytotoxicity.

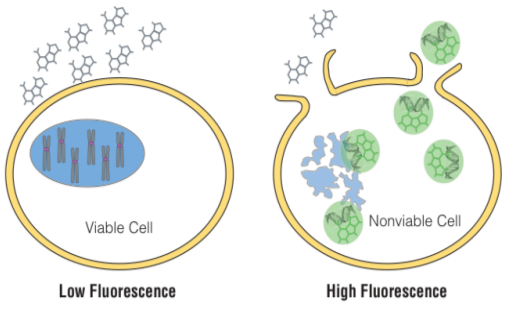

Figure 10: CellTox-Green Dye binds DNA of cells with impaired membrane integrity (Promega, 2015)

The cells were seeded out in white 96-well plates with 15 000 cells/well (SW620), and 8 000 cells/well (HCT116) in 50µl/well with 10µl CellToxGreen Dye per 5 ml cell suspension. After 24 hours the cells were treated with different inhibitors at concentration of 0.4µM, 2µM and

10µM. The fluorescence was measured using PolarStarOmega (Excitation λ=485nm, Emission λ=520nm) (BMG Labtech) after several time-points (0h, 2h, 4h, 6h, 24h, and 48h.)

We used three different controls for this assay: Toxicity control (positive control), negative control (untreated cells) and background control. The toxicity control is performed by adding lysis solution before the last readout (48h) and represents the maximum signal obtainable. Control wells with medium and reagent only were used to determine the background noise.

2.4 CASPASE-GLO 3/7 ASSAY

Caspase-Glo 3/7 Assay (Promega, #280789) is a luminescence assay that measures caspase 3 and 7 activities (Promega, 2016). The reagent contains a luminogenic caspase 3/7 substrate. The addition of the reagent results in cell lysis followed by caspase cleavage of the substrate and generation of a luminescent signal produced by luciferase (Figure 11). The luminescent signal is proportional to the caspase activity (Promega, 2016).

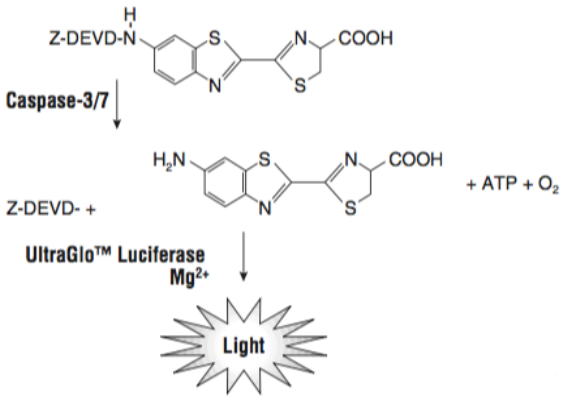

Figure 11: Caspase 3 and 7 cleaves off the DEVD tetrapeptid from the substrate, and luciferase generates a luminescent signal (Promega, 2016).

The cells were seeded out in white 96-well plates with 15 000 cells/well (SW620) and 8000 cells/well (HCT116) in 100µl/well, respectively. After 24 hours of incubation the cells were treated with different inhibitors at concentration of 0.4µM, 2µM and 10µM for 24 hours or 48 hours. After 24 or 48 hours the caspase 3/7 reagent was added and incubated on a shaker (300 rpm) in room temperature for 2h to facilitate cells lysis. Luminescence was assessed using Wallac VICTOR 1420 Multilabel counter (PerkinElmer). Two different controls were used for this assay: Negative control (untreated cells) and background control.

2.5 CONFLUENCY ASSESSMENT

The cells seeded out for the assay CelltoxGreen were imaged on EVOS (ThermoFisher Scientific) after 24h and 48h inhibitor incubation, with bright field to measure cell confluency. The program "Cellprofiler" were used to quantify confluency. How the program analyzed the pictures in shown in Figure 12. In the enhanced image the lowest grey values are changed to black. In the binary image the highest grey values are changed to white. In this case the background is colored black and the cells are colored white. The program then measures the black and the white area, respectively.

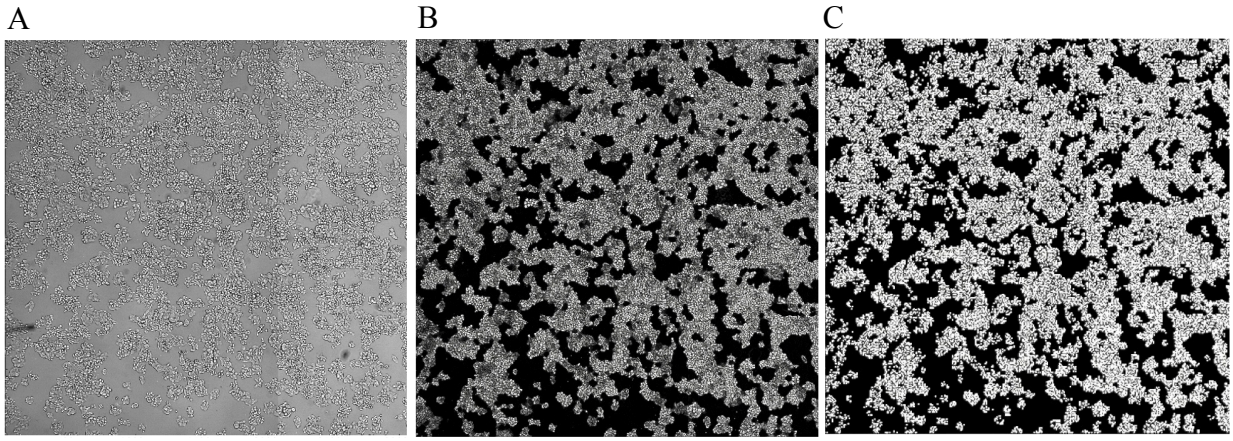

Figure 12: Confluency assessment. A: Original image. B: Enhanced image. C: Binary image.

The confluency assessment was performed on both cell lines (SW620 and HCT116). "Feature size" was defined as the diameter of the cell and helps the program to analyze the pictures. The value for SW620 were 25 and for HCT116 the value was 80.

2.6 REPORTER KIT ASSAY

The "Cignal Finder Reporter Array" (Qiagen, #7511300245) was used and the experiment was performed as follows:

Day 1: HCT116 and SW620 cells were split in a ratio of 1:2.

Day 2: The cells were seeded out in white 96-well plate with 20 000 cells/well (SW620 and HCT116) in 100µl/well and incubated for 24 hours, respectively.

Day 3: Media containing antibiotic and serum was aspirated, and cells were washed with antibiotic and serum-free media, followed by addition of 50µl of antibiotic and serum free media per well. The transfection mix was prepared according to Biontex protocol: 0.08µg DNA and 0.6µl Metafectene Pro (Metafectene Pro, Biontex, #ASP201/RK121216) (SW620 cells) and 0.1µg DNA and 0.4µl Metafectene Pro

(HCT116 cells), were diluted in separate tubes in 25 µl antibiotic and serum-free media, respectively. The diluted DNA was subsequently transferred into the tube containing the diluted transfection reagent and incubated at room temperature for 15-20 min. 50µl of DNA-lipid complexes were added dropwise to the cells and incubated for 4.5 h. After the incubation time, the transfection media was removed, and the cells were further cultivated in 100µl of complete growth media until the next day.

Day 4: The transfection efficiency was evaluated through the positive green fluorescent protein (GFP) control with EVOS (ThermoFisher Scientific). Cells were treated with different inhibitors at a concentration of 2µM for 6 hours. 75µl of media was then removed and 75µl DualGlo reagent (Dual-Glo luciferase assay system, Promega, #245577) added. The plate was transferred to shaker (600 rpm, room temperature) to aid the cells lysis. Firefly luciferase was then measured. 75µl Dual Glo Stop&Go reagent (Dual-Glo luciferase assay system, Promega, #245577) was added to each well and incubate for 10 minutes on the shaker. Renilla luciferase was then measured. Firefly and Renilla was detected using Wallac VICTOR 1420 Multilabel counter (PerkinElmer).

The positive control serves as a control for transfection efficiency, by monitoring GFP expression, as well as a positive control for both the Firefly and Renilla luciferase assays. A negative control was also included and works as a specificity control.

3. RESULTS

3.1 THE EFFECT OF INHIBITORS ON PHOSPHO-PROTEINS

In our initial high throughput study, we observed that the combinations GSK3 inhibitor (CT) + p90RSK inhibitor (D1) and PI3K inhibitor (PI) + D1 had an increased negative effect on viability in SW620 cells, compared to either of the inhibitors alone (Figure 5). Next, we wanted to examine the impact of these single inhibitors on their targets protein activity.

SW620 and HCT116 cells were treated with the three inhibitors for 24h, and phosphoproteins were determined by immunoblot (Figure 13). We found that the PI3K inhibitor PI reduced the phosphorylation of p-AKT Ser473 in both cell lines. This corresponds with previous findings in these cell lines (Fernandez, 2009; Potter, 2014). Treatment of SW620 and HCT116 cells with the GSK3α/β inhibitor CT increased phosphorylation of GSK3α. In contrast, the p90RSK inhibitor D1 did not affect the phosphorylation status of BAD on Ser112 in either of the cell lines. The inhibitors did not affect the total protein.

Immunoblot is a semi-quantitative method. These results may be explained by the detection level of the method, off-target effects of the inhibitors and/or more likely crosstalk between intracellular pathways. We concluded that by this method it is difficult to assess the effect of different inhibitors.

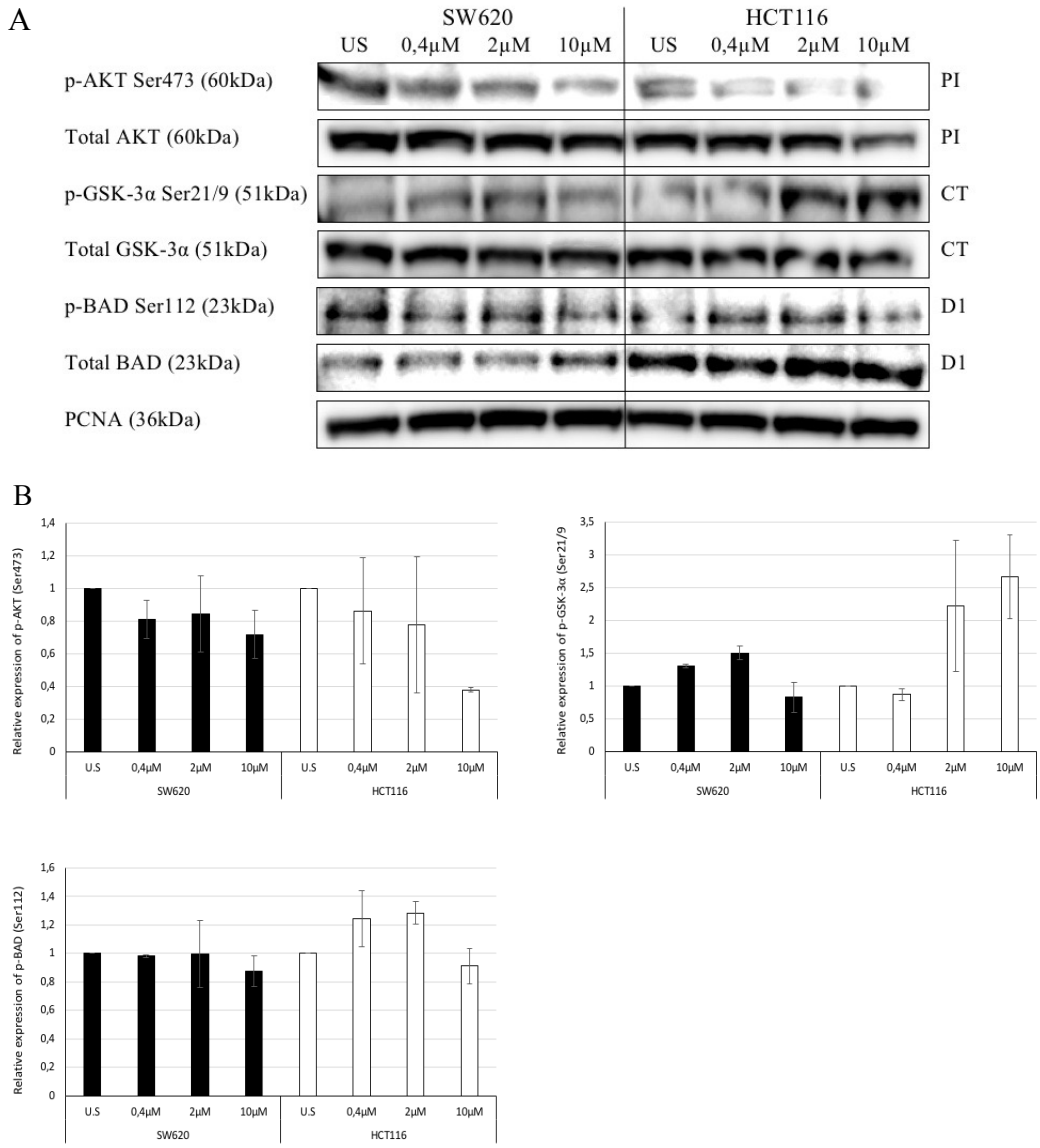

Figure 13. A: Immunoblot of SW620 and HCT116 cells treated with inhibitors at a concentration of 0.4, 2 and 10µM for 24h. (PI:PI3K inhibitor, CT:GSK3 inhibitor, D1:p90RSK inhibitor). B: Relative expression. PCNA was used for normalization. (n=2). Total protein, expect PCNA n=1.

3.2 CELL MORPHOLOGICAL CHANGES

Cell death can be classified according to its morphological appearance; like cell shrinkage, membrane blubbing and DNA- and cell fragmentation (Kroemer, 2009). Thus, we ask the question whether we are able to investigate the inhibitors effect on these cell morphology changes.

SW620 and HCT116 cells were treated with the inhibitors with various concentrations (0.4, 2 and 10µM) in single and in combination for 48 hours. The morphology changes were

determined by microscopy images. We did not observe any cellular changes in SW620 cells exposed to 0.4μM of any of the tested inhibitors. With increased concentration, however, we noticed membrane blebbing in SW620 cells treated with 2μM (data not shown) and 10μM of the PI inhibitor (Figure 14, B). A similar effect was observed upon treatment with the inhibitor D1. Additionally, cell fragmentation was observed (Figure 14, C). The CT inhibitor, however, did not influence the cell morphology (Figure 14, D).

Further, we investigated if treatment with inhibitor combinations increased the effect on cell morphology compared to both single treatments. In SW620 cells treated with the inhibitor combinations PI+D1 (Figure 14, E) and PI+CT (Figure 14, F), we did not observe any additional effect. The inhibitor combinations D1+CT (Figure 14, G), showed additionally to membrane blebbing, increased cell fragmentation, compared to either of the inhibitors alone.
In conclusion, we found that both PI and D1 inhibitor affects cell morphology. Increased effect was observed with the combined inhibitors D1+CT compare to either of the inhibitors alone.

We observed that HCT116 cells showed the same pattern as SW620 cell (Appendix 2).

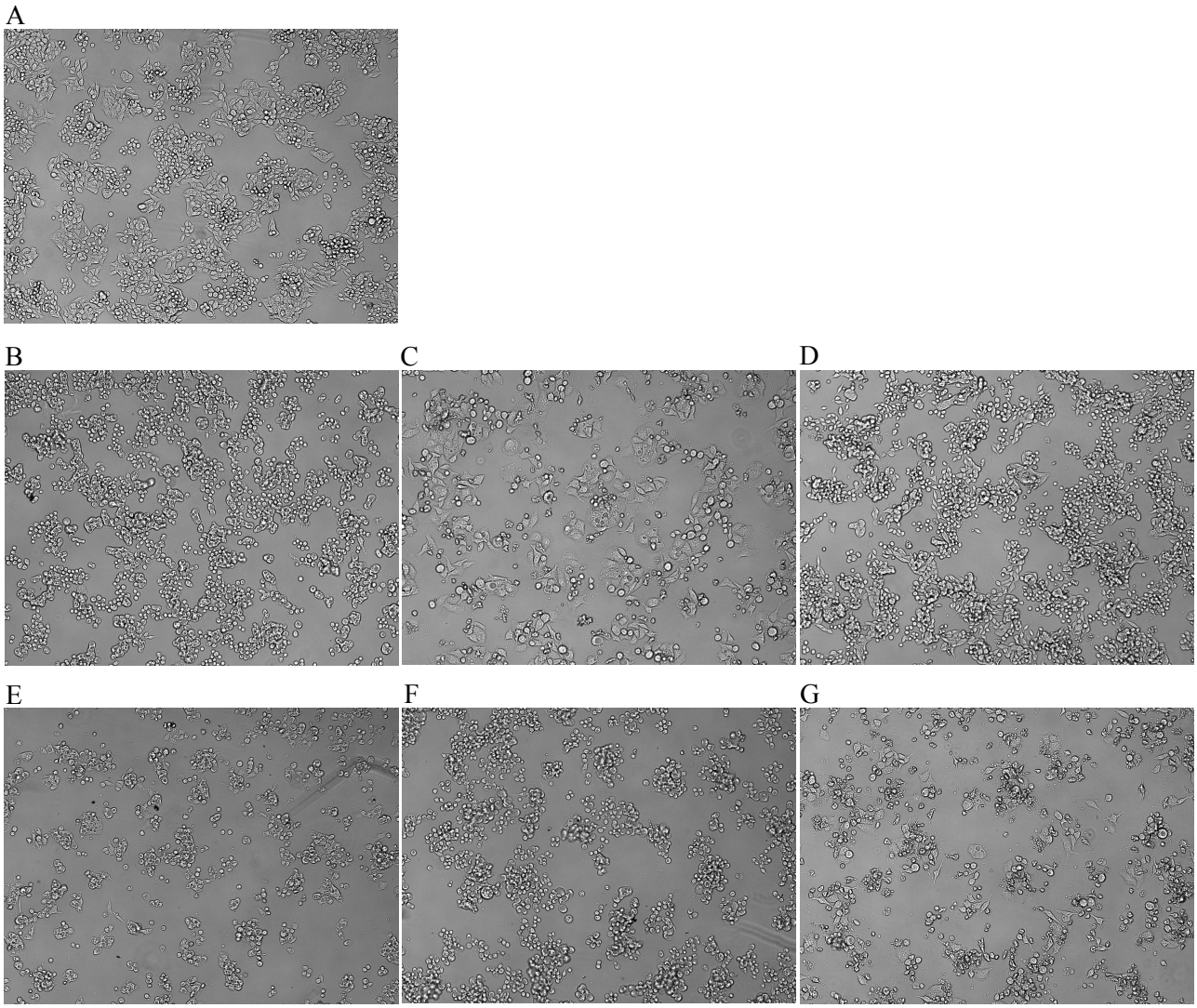

Figure 14: Microscopy images of SW620 cells treated with inhibitors at a concentration of 10μM for 48h(10x). A: Untreated cells. B: PI:PI3K inhibitor. C: D1:p90RSK inhibitor. D: CT:GSK3 inhibitor. E: PI+D1:PI3K+p90RSK inhibitors. F: PI+CT:PI3K+GSK3 inhibitors. G: D1+CT:p90RSK+ GSK3 inhibitors.

3.3 CELL DEATH DETECTION

Since we observed membrane blebbing and cell fragmentation of SW620 and HCT116 cells treated with inhibitors indicating that they induce cell death, we further wanted to confirm this by performing a cell death assay. Therefor we performed CellTox Green assay, which continuously measures reduction in cell membrane integrity, a result of cell death.

SW620 and HCT116 cells were treated with inhibitors in single and in combinations with different concentration up to 48 hours. We observed decreased caspase activity in SW620 cells treated with PI compared to the control (Figure 15, A). Treatment with 10μM of the single inhibitors D1 and CT showed significant increased cell death compare to the control (*) (Figure

15, B and C). Combination of PI+D1 and PI+CT seems to block the previously observed effect of D1 and CT on cell death (Figure 15, D and E). Treatment with the inhibitor combination D1+CT we observed a synergetic effect (Figure 15, F). The synergetic effect corresponds with observed morphological changes.

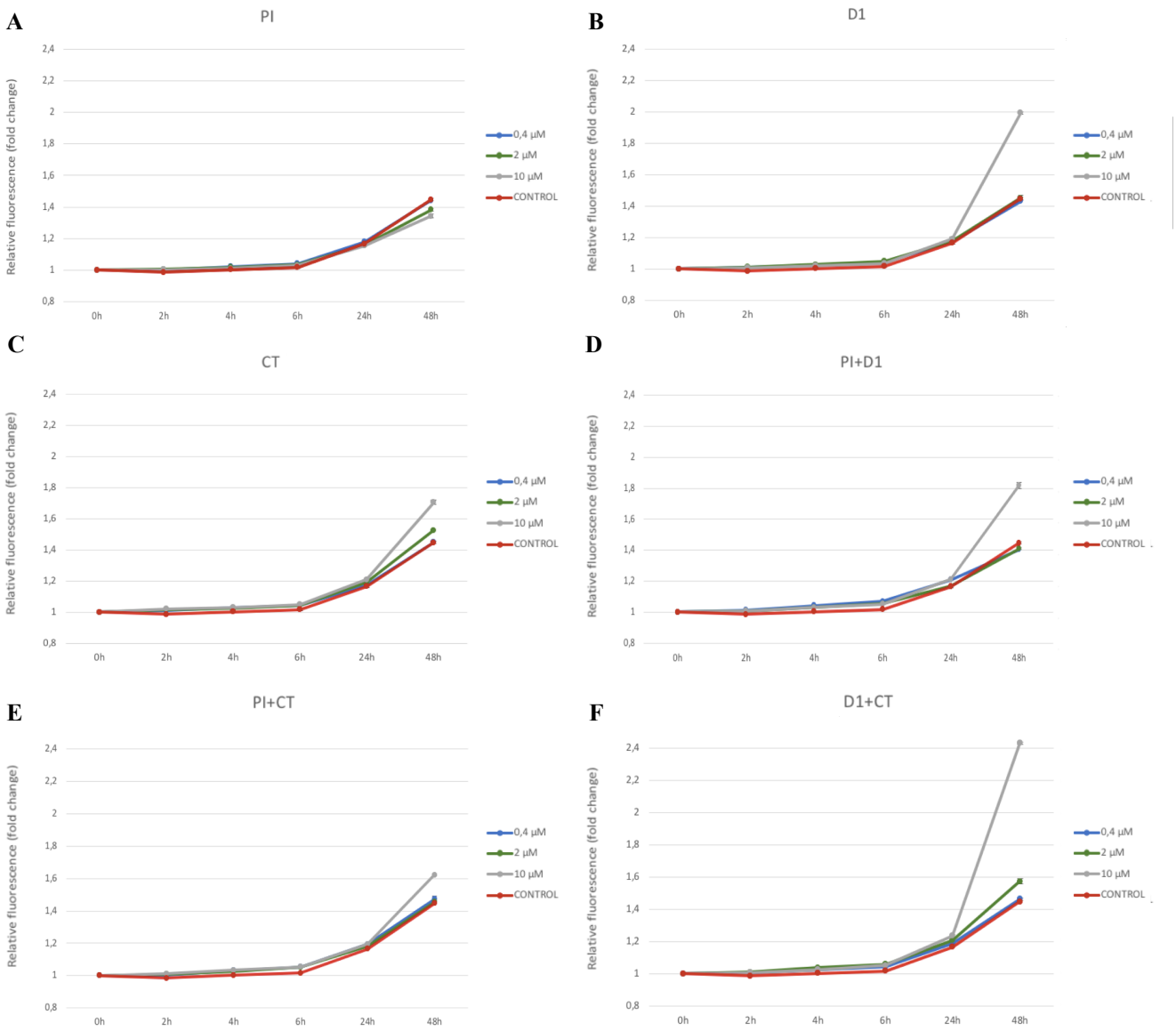

Figure 15: Cell death in SW620 cells treated with inhibitors at a concentration of 0.4, 2 and 10µM up to 48h. A: PI:PI3K inhibitor. B: D1:p90RSK inhibitor. C: CT:GSK3 inhibitor. D: PI+D1:PI3K+p90RSK inhibitors. E: PI+CT:PI3K+GSK3 inhibitors. F: D1+CT:p90RSK+ GSK3 inhibitors. n=3. Statistic were obtained from two-tailed student t-test. p-value: *<0.05, **<0.01. The cutoff for synergy was HSA < -0.12.

In HCT116 cells treated with 10µM of the single inhibitor D1 showed significant increased effect compare to the control (*) (Figure 16, B). Treatment with the inhibitor combination D1+CT showed synergetic effect (Figure 16, F). These results correspond with observed morphological changes.

To conclude, both cell lines showed synergetic effect on cell death with the inhibitor combination D1+CT.

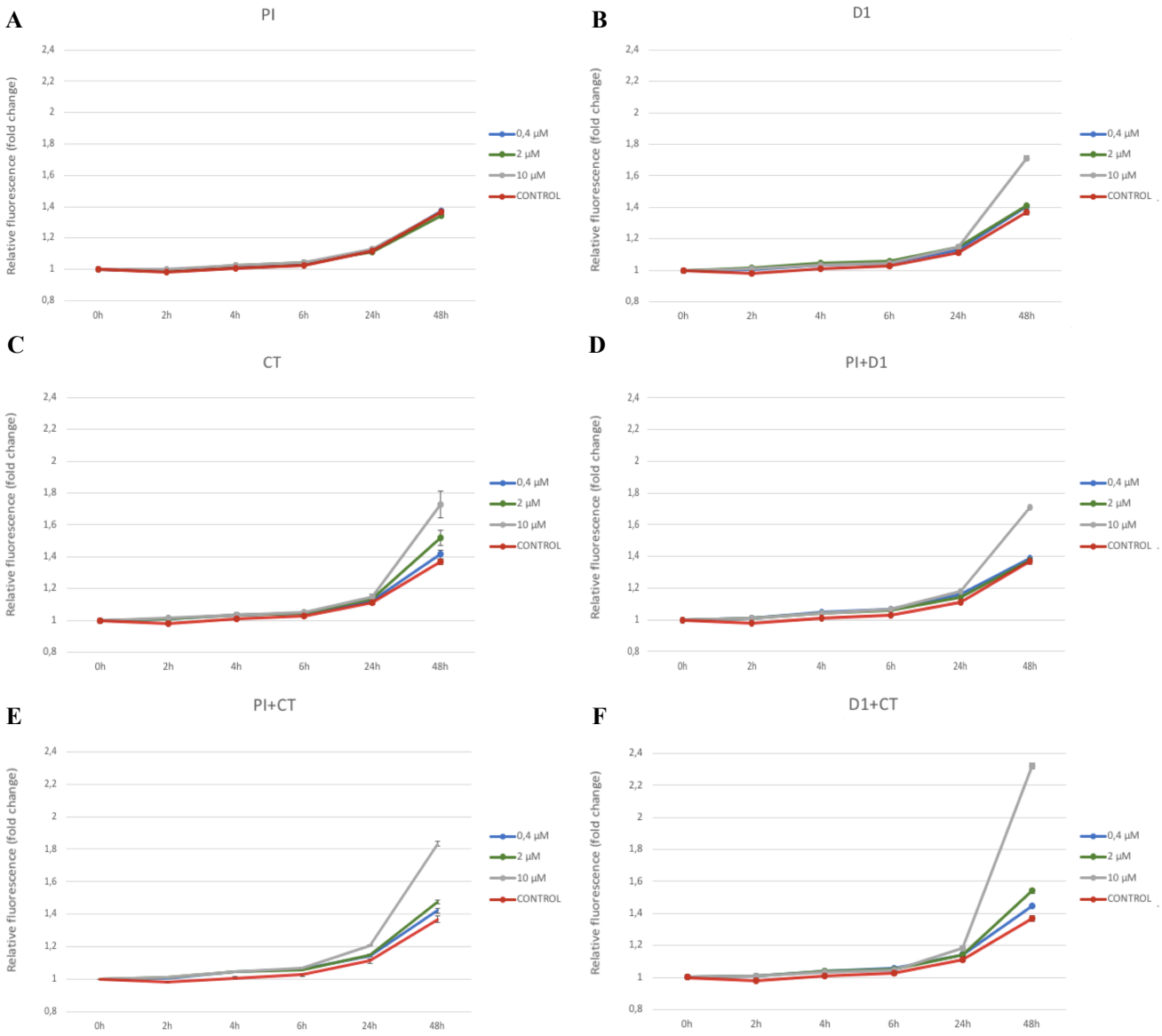

Figure 16: Cell death in HCT116 cells treated with inhibitors at a concentration of 0.4, 2 and 10µM up to 48h. A: PI:PI3K inhibitor. B: D1:p90RSK inhibitor. C: CT:GSK3 inhibitor. D: PI+D1:PI3K+p90RSK inhibitors. E: PI+CT:PI3K+GSK3 inhibitors. F: D1+CT:p90RSK+ GSK3 inhibitors. n=3. Statistic were obtained from two-tailed student t-test. p-value: *<0.05, **<0.01. The cutoff for synergy was HSA < -0.12.

3.4 CASPASE ACTIVITY

Cell death has been historically classified into three different types; apoptosis, autophagy and necrosis (Kroemer, 2009). Most of the key players in cellular apoptosis regulation are identified and can be targeted by therapeutic strategies (Fischer, 2006). Thus, we wanted to examine whether apoptosis was involved in the observed cell death.

SW620 and HCT116 cells were treated with inhibitors in single and double application with various concentration for 24 or 48 hours, and caspase activity were determined by the Caspase-Glo 3/7 assay. We observed decreased caspase activity in SW620 cells treated with PI compared to the control (Figure 17). Treatment with the single inhibitors D1 and CT showed significant increased apoptosis compare to the control. Combination of PI+D1 and PI+CT seems to block the previously observed effect of D1 and CT on apoptosis. The inhibitor combination D1+CT had a synergetic effect at concentration 10µM. These results, correspond with the CellTox Green assay and reveal that apoptosis was involved.

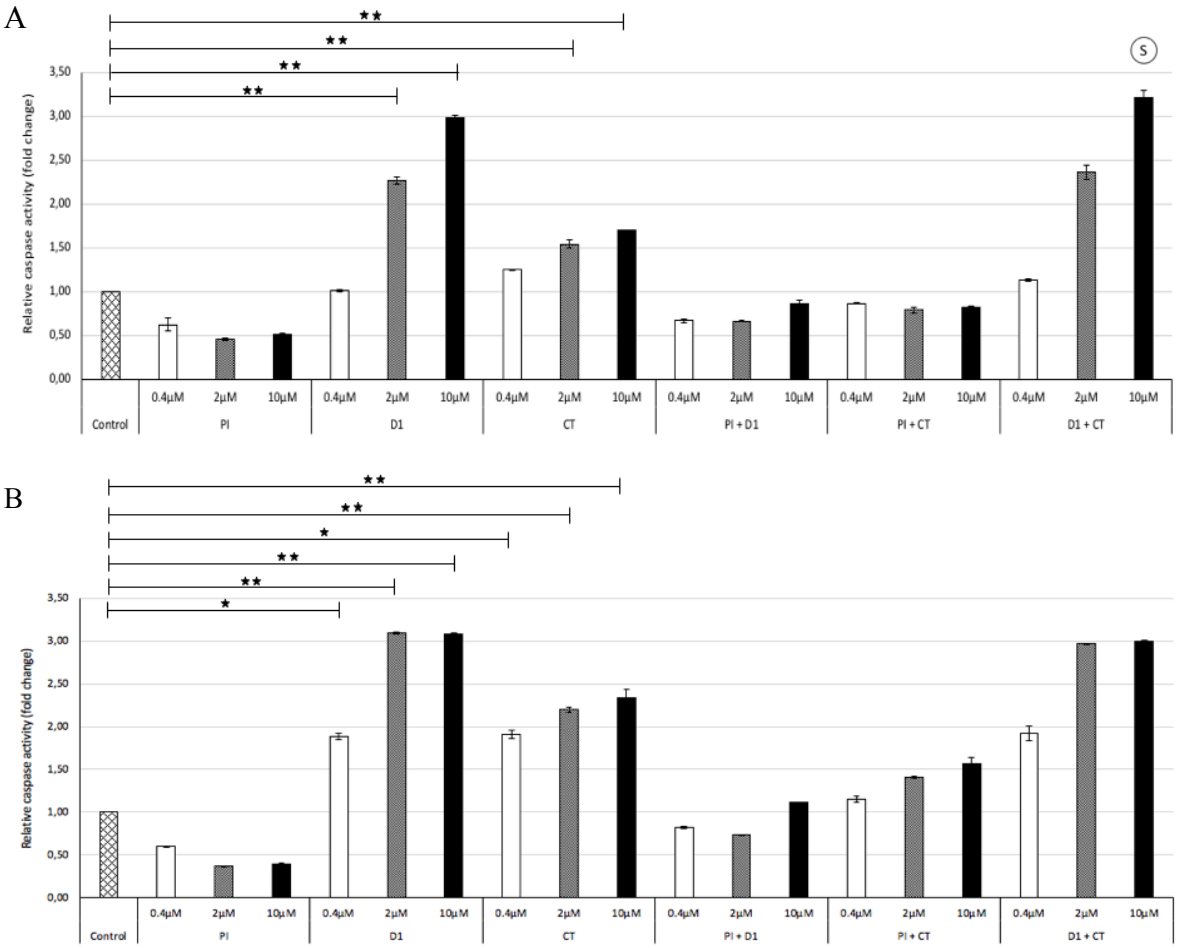

Figure 17: Caspase activity in SW620 cells treated with inhibitors at a concentration of 0.4, 2 and 10µM for 24h or 48h. PI:PI3K inhibitor, D1:p90RSK inhibitor and CT:GSK3 inhibitor. A:24h. B:48h. n=3. Statistic were obtained from two-tailed student t-test. (p-value: *<0.05, **<0.01) The cutoff for synergy was HSA < -0.12.

The same results were observed in HCT116 cells (Figure 18). Additionally, in HCT116 cells the inhibitor combination D1+CT had a synergetic effect in all concentrations.

To conclude, both cell line showed synergetic effect on apoptosis with the inhibitor combination D1+CT. These results, correspond with the CellTox Green assay and reveal that apoptosis was involved.

A

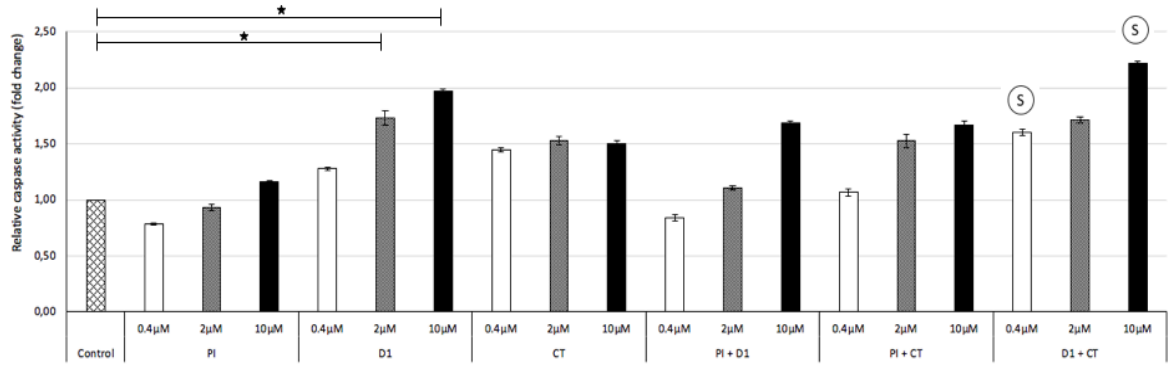

B

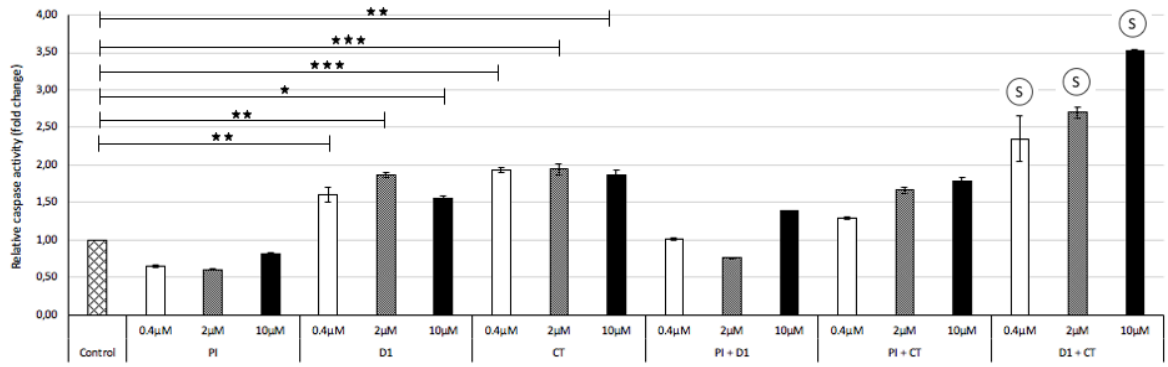

Figure 18: Caspase activity in HCT116 cells treated with inhibitors at a concentration of 0.4, 2 and 10µM for 24h or 48h. PI:PI3K inhibitor, D1:p90RSK inhibitor and CT:GSK3 inhibitor. A:24h. B:48h. n=3. Statistic were obtained from two-tailed student t-test. (p-value: *<0.05, **<0.01) The cutoff for synergy was HSA < -0.12.

3.5 CONFLUENCY ASSESSMENT

Drug treatment may affect the cell proliferation through different signal transduction pathways (Zhang, 2013). Therefor it was also of interest to assess confluency to observe the inhibitors effect on proliferation, referring to the number of adherent cells in culture wells.

SW620 and HCT116 cells were treated with inhibitors in single and in combination for 24h or 48 hours. The confluency assessment was determined by imaging and the Cellprofiler program. SW620 cells treatment with single PI inhibitor showed significant decreased proliferation compare to the control (Figure 19). The inhibitor combination PI+D1 showed synergistic effect.

A

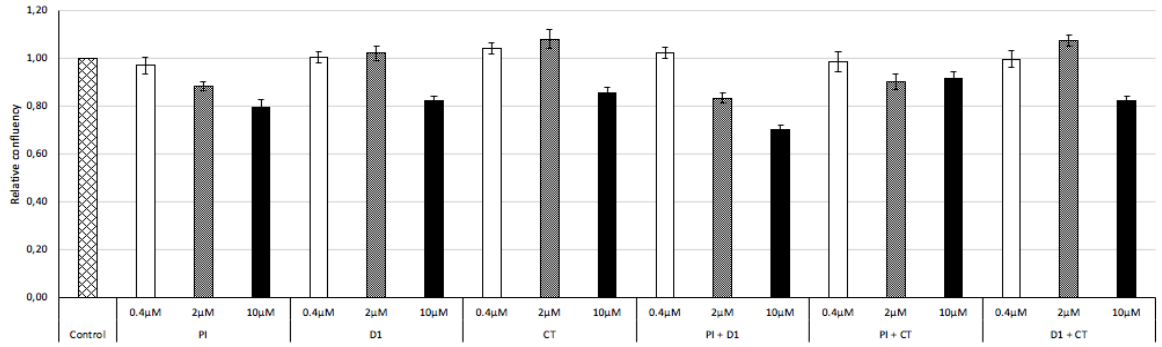

B

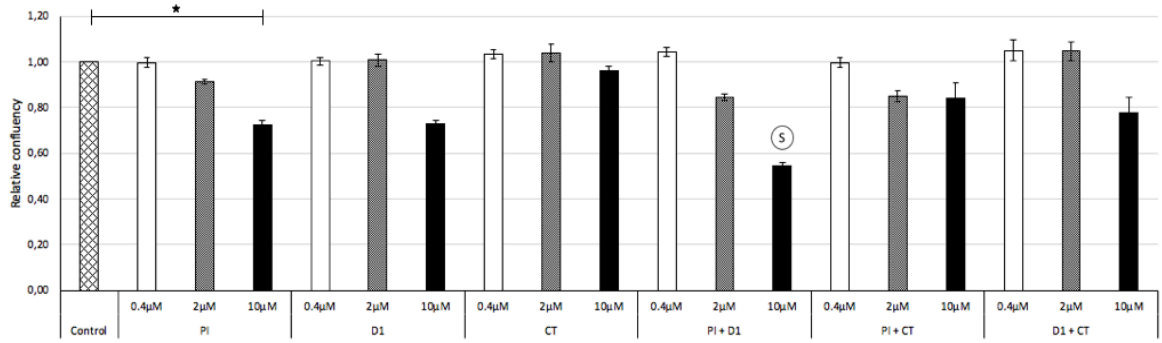

Figure 19: Confluency assessment of SW620 cells treated with inhibitors at a concentration of 0.4, 2 and 10µM for 24h or 48h, PI:PI3K inhibitor, D1:p90RSK inhibitor and CT:GSK3 inhibitor. A:24h. B:48h. n=3. Statistic were obtained from two-tailed student t-test. (p-value: *<0.05, **<0.01) The cutoff for synergy was HSA < -0.12.

The cell line HCT116 also showed significant decreased proliferation in treatment with single PI inhibitor compare to the control, but no synergetic effect was found (Figure 20).

A

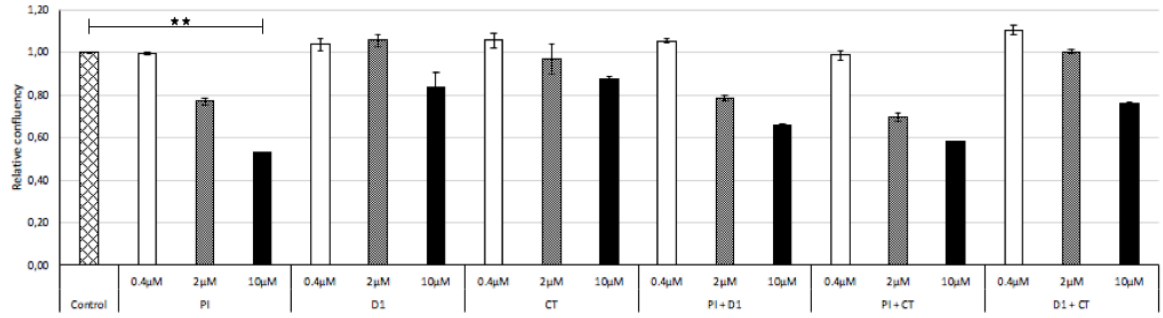

B

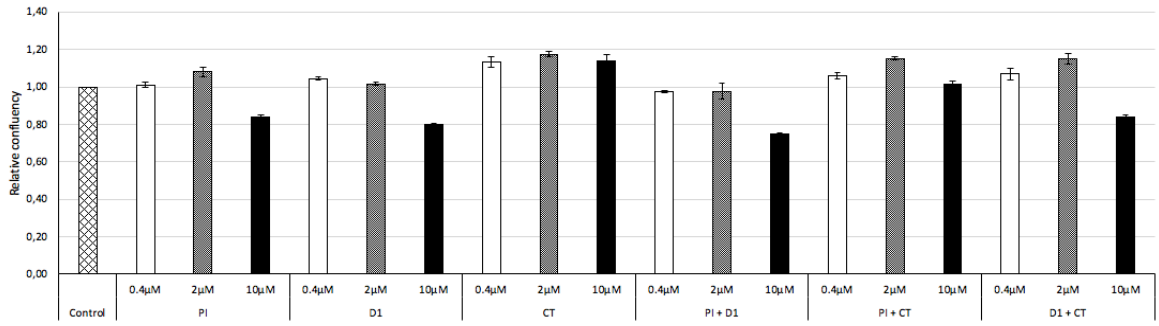

Figure 20: Confluency assessment of HCT116 cells treated with inhibitors at a concentration of 0.4, 2 and 10µM for 24h or 48h, PI:PI3K inhibitor, D1:p90RSK inhibitor and CT:GSK3 inhibitor. A:24h. B:48h. n=3. Statistic were obtained from two-tailed student t-test. (p-value: *<0.05, **<0.01) The cutoff for synergy was HSA < -0.12.

3.6 REPORTER GENE ASSAY

Intracellular signaling often leads to activation of transcription factors and gene expressions. We ask the question whether the inhibitors will affect the transcriptional activation of transcription factors involved in cell proliferation and survival.

3.6.1 OPTIMIZATION OF REPORTER KIT

Initially we established the transfection procedure for CRC cell lines (SW620 and HCT116) using the GFP plasmid, provided in the kit (Promega), as positive control. Cells were seeded and transfected as described under material and methods, paragraph 2.6. The transfection was check by GFP plasmid using imaging.

These results showed that seeding of 25 000 cells/well, resulted in low transfection efficacy, approximate 5-10%, in SW620 cells (Figure 21, B). Additionally, we observed a high number of cells that were lumped together and lying on top of each other (Figure 21, A). In the protocol the manufacturer recommends that at the day of transfection the cells should preferably be around 50% confluent or less. Thus, we investigated if the transfection efficacy would increase by seeded out a lower number of cells per well. We observed that seeding of 20 000 cells/well

resulted in a slightly increased transfected efficacy (Figure 21, D). However, still only 10-15% of cells were transfected with the plasmid. We concluded that SW620 cells were difficult to transfect by this method and no further experiments was performed with these cells.

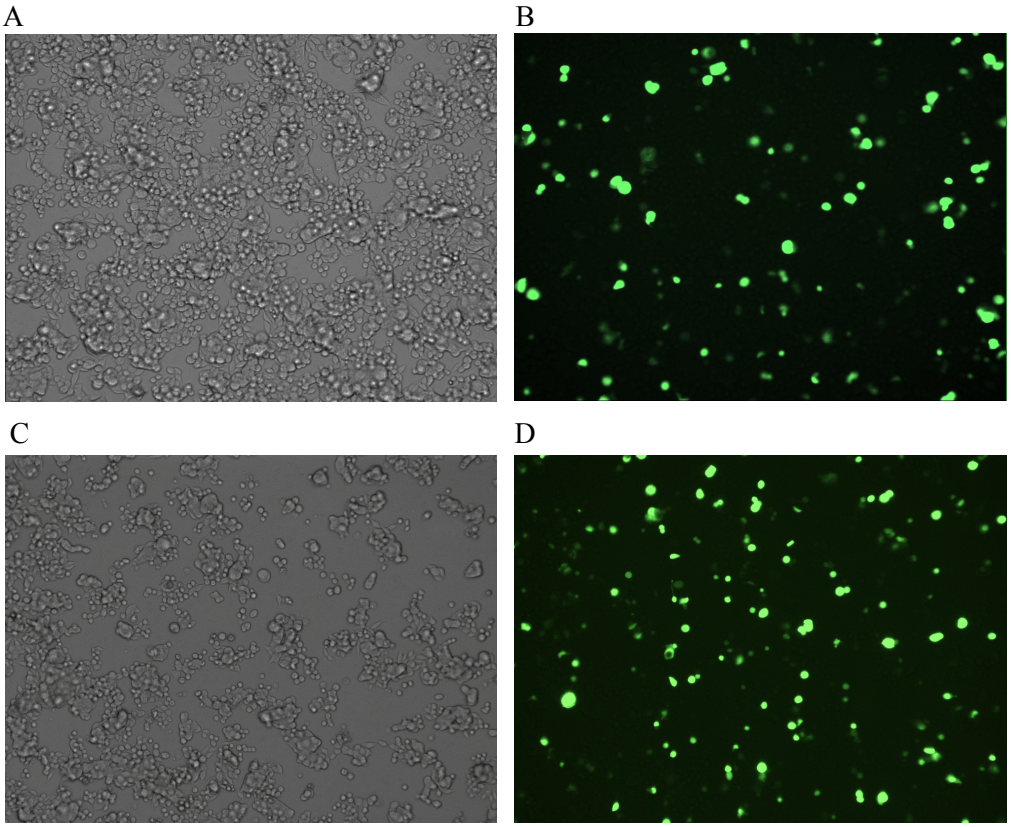

Figure 21: Transfection of SW620 cells. A and B: 25 000 cells/well. C and D: 20 000 cells/well. Left: Trans image. Right: GFP image. (10x)

In HCT116 cells a transfection efficiency of approximately 80% was observed (Figure 22). Further experiments where therefor performed only in HCT116 cells.

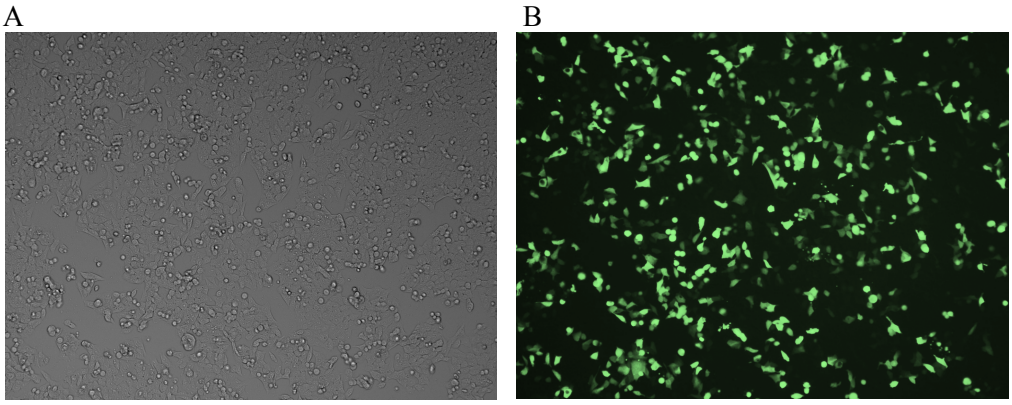

Figure 22: Transfection of HCT116 cells with 20 000 cells/well. A: Trans image. B: GFP image. (10x)

3.6.2 TRANSCRIPTIONAL ACTIVATION OF MYC AND E2F

The transcription factor MYC and E2F are both effecting the gene expression for cell proliferation (Cascón, 2012; Ozono, 2013). The confluency assessment showed decreased proliferation in treatment with PI inhibitor in HCT116 cells. Thus, we ask the question whether the inhibitors would affect the transcriptional activation of these specific transcription factors.

HCT116 cells were treated with PI, D1 and CT in single and double application at 2µM for 6h (Figure 23). The relative luciferase of the transcription factor MYC and E2F is down regulated in cells treated with PI alone and in combination with D1 and CT. The results indicate that inhibition of PI3K using PI may prevent cell proliferation through down regulated transcriptional activation of the transcription factor MYC and E2F.

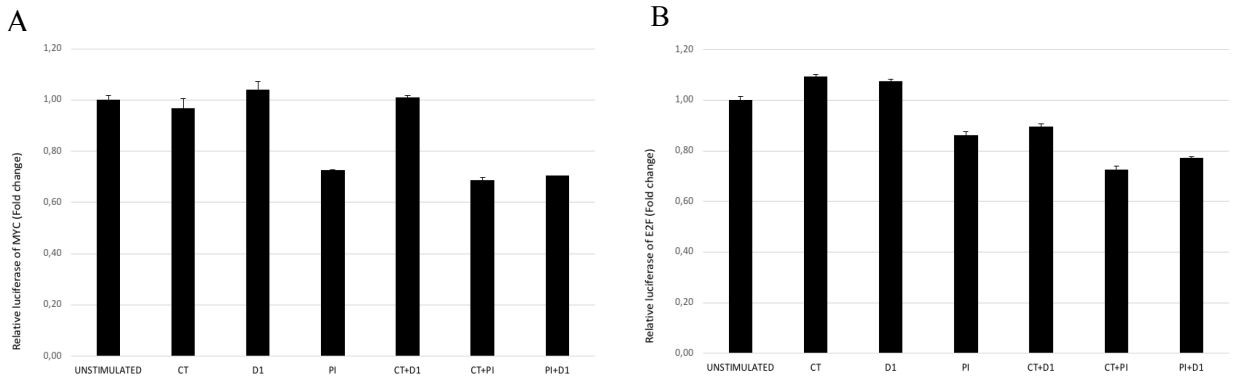

Figure 23: Transcription activity in HCT116 cells treated with inhibitors at a concentration of 2µM for 6h. A: Relative luciferase of the transcription factor MYC. B: Relative luciferase of the transcription factor E2F. PI:PI3K inhibitor, D1:p90RSK inhibitor and CT:GSK3 inhibitor. (n:2).

4. DISCUSSION

Combinatory drug treatment tailored to an individual's tumor is expected to overcome problems related to individual variation in drug efficacy, resistance and side effect (Al-Lazikani, 2012; Collins, 2015). Our research group has performed a high throughput screening on multiple cell line to discover synergetic drug combinations. The aim of this study was to evaluate and characterize the effect of specific inhibitor combinations initially observed by high throughput screening further and to study the effect of these combinations on another CRC cell line.

The D1 inhibitor in single treatment induced high cell death and apoptosis in both cell lines. This may indicate that RAS-MAPK-ERK pathway plays a central role in these cell lines. SW620 and HCT116 cells harbor a KRAS mutation (Cancer Cell Line Encyclopedia (CCLE), 2018), which results in a constative activation of the RAS-MAPK-ERK pathway that promotes cell survival. Treatment with the D1 inhibitor hampers the downstream pathway and lead to cell death. Mendoza et. al. stated that BAD induces apoptosis by neutralizing the pro-survival BCL2 protein family. p90RSK inhibits BAD by phosphorylation that promotes cell survival by sequestering BAD in the cytosol, away from pro-survival BCL2 family members (Mendoza, 2011). These findings may explain the observed apoptosis and cell death by inhibition of p90RSK (D1).

The CT inhibitor in single treatment also induced high cell death and apoptosis in both cell line. The mechanisms of GSK3 regulation are varied and not fully understood but McCbrey et. al. stated that GSK3 stabilizes the expression of certain anti-apoptotic Bcl-2 family members (McCubrey, 2014). GSK3 also plays an important role in the Wnt/beta-catenin pathway. McCbray et. al. stated that GSK3 has oncogenic properties by stabilizing components of the beta-catenin complex (McCubrey, 2014). These findings may explain the observed apoptosis and cell death by inhibition of GSK3 (CT).

The PI inhibitor did not influence cell death or caspase activity in either of the cell line. This is in accordance with other findings, that also observed that treatment with PI3K inhibitor (PI) did not results in apoptosis in CRC cell line, SW620 and HCT116 (Potter, 2014; Raynaud, 2007). However, we did observe that PI decreased proliferation in both cell lines. In HCT116 cells we further observed a down regulated transcriptional activation of the transcription factors MYC and E2F. These two transcription factors are both affecting the gene expression for cell proliferation (Cascón, 2012; Ozono, 2013). Cascon at. al. observed that MYC promotes

oncogenic transformation and tumorigenesis by activation the transcription of target genes that drive cell proliferation and stimulate angiogenesis (Cascón, 2012). Ozono at. al. found that the E2F transcription factors control cell proliferation by regulating the expression of genes whose products are required for S phase entry and progression (Ozono, 2013). The findings of down regulated transcriptional activation of these transcription factors with treatment of the PI inhibitor may indicate a cytostatic effect and inhibition of the PI3K-AKT pathway may prevent cell proliferation.

The high throughput screening show that the inhibitor combination CT+D1 and PI+D1 are synergistic for the cell line SW620. SW620 cells treated with the inhibitor combination CT+D1 had a synergetic effect on apoptosis and cell death. This inhibitor combination was also most effective when it comes to morphological changes. Additionally, we observed synergetic effect on decreased proliferation with the inhibitor combination PI+D1, which indicated that D1 may also have an effect on proliferation. These results correspond with the high-throughput screening. Treatment with the inhibitor combinations CT+D1 also had a synergetic effect on apoptosis and cell death in the cell line HCT116.

The inhibitors are not in clinical use and no articles showing the combinatorial effect of these inhibitors have been published. However, several papers demonstrate that the effect of combined inhibitors that blocks both the PI3K-mTOR pathway and the MAPK-ERK-pathway, increase anti-proliferative effects and apoptosis, compare to single inhibitor treatment (Halilovic, 2010; Pitts, 2014; Roper, 2014; Ye, 2014). Pitts et. al. observed with in vitro experiments that the combination of PI3K and MEK inhibitor showed synergistic anti-proliferative activity, compare to single treatment in CRC cells. Enhanced reduction in tumor growth was also observed in vivo with this combined treatment (Pitts, 2014). Roper et.al. demonstrated that combination PI3K and MEK inhibition promotes apoptosis and tumor regression in mouse models of colorectal cancers (Roper, 2014).

As mentioned above SW620 cell showed synergy effect on decreased proliferation with the inhibitor combination PI+D1. This synergy was not found in HCT116 cell, but we observed a decreased effect on proliferation compare to both the single inhibitor. Other differences are that the cell line HCT116 is a primary cell line (human colorectal carcinoma) while the cell line SW620 is from a metastatic site (human colorectal adenocarcinoma). This may reflect the observed synergetic effect on apoptosis in HCT116 cell. The HCT116 cells showed synergy

with the inhibitor combinations CT+D1 at all concentration, while the SW620 cells showed synergy only at a concentration of 10μM. Luo et. al. stated that chemotherapy insensitivity and poor prognosis are biological characteristics of metastases CRC. They observed that the ability of drug resistant in metastatic cells SW620 was greater than primary colorectal cancer cells SW480 (Luo, 2016).

5. CONCLUSION

To conclude, the inhibitor combination CT+D1 showed synergetic effect on apoptosis activity and cell death in the SW620 cell line. In addition, PI+D1 showed synergetic effect on decreased proliferation. These finding were corresponding to the high throughput screening. The inhibitor combination CT+D1 were also synergetic in the HCT116 cell line. These inhibitor combinations could be an interesting treatment approach.

6. REFERENCES

- Al-Lazikani, B., Banerji, U., Workman, P. (2012). - Combinatorial drug therapy for cancer in the post-genomic era. *Nat Biotechnol, 30*(7), 679-692.
- Alberts, B. (2009). Essential cell biology. *Third edition ed. USA: Garland science, Taylor and Francis group.*
- Cancer Cell Line Encyclopedia (CCLE). (2018). www.broadinstitute.org/ccle. *The Broad Institute of MIT & Harvard*.
- Carracedo, A., Ma, L., Teruya-Feldstein, J., Rojo, F., Salmena, L., Alimonti, A., Egia, A., Sasaki, A.T., Thomas, G., Kozma, S.C., Papa, A., Nardella, C., Cantley, LC., Baselga, J., Pandolfi, P.P. (2008). - Inhibition of mTORC1 leads to MAPK pathway activation through a PI3K-dependent. *J Clin Invest, 118*(9), 3065-3074.
- Cascón, A., Robledo, M. (2012). MAX and MYC: A Heritable Breakup. *American Association for Cancer Research*, pp. 3119-3124.
- Cathomas, G. (2014). PIK3CA in Colorectal Cancer. *Front Oncol*.
- Chaussepied, M., Ginsberg, D. (2004). - Transcriptional regulation of AKT activation by E2F. *Mol Cell, 16*(5), 831-837.
- Collins, F. S., Varmus, H. (2015). - A new initiative on precision medicine. *N Engl J Med, 372*(9), 793-795.
- Danielsen, S. A., Eide, P.W., Nesbakken, A., Guren, T., Leithe, E., Lothe, R.A. (2015). Portrait of the PI3K/AKT pathway in colorectal cancer. *Biochimica et Biophysica Acta (BBA) - Reviews on Cancer*.
- Elmore, S. (2007). Apoptosis: A review of programmed cell death. *Toxicol Pathol*, 35(34):495-516.
- Fang, J. Y., Richardson, B.C. (2005). The MAPK signalling pathways and colorectal cancer. *Lancet Oncol, 6*(5), 322-327.
- Ferlay, J., Soerjomataram, I., Dikshit, R., Eser, S., Mathers, C., Rebelo, M., Parkin, D.M., Forman, D., Bray, F. (2015). - Cancer incidence and mortality worldwide: sources, methods and major patterns in. *Int J Cancer, 136*(5), 9.
- Fernandez, M. C., Bales, J., Hodgkinson, C., Welman, A., Welham, M.J., Dive, C., Morrow, C.J. . (2009). Blocking PI3-Kinase Activity in Colorectal Cancer Cells Reduces Proliferation but does not Increase Apoptosis Alone or in Combination with Cytotoxic Drugs. *Molecular Cancer Research : MCR, 7(6), 955–965.*
- Fischer, U., Schulze-Osthoff, K. (2006). Apoptosis-based therapies and drug targets. *Cell Death and Differentiation, 16(1), 3–11.*
- Foucquier, J., Guedj, M. (2015). Analysis of drug combinations: current methodological landscape. *Department of Bioinformatics and Biostatistics.* .
- Gómez-Sintes, R., Hernández, F., Lucas, J.J., Avila, J. (2011). GSK-3 Mouse Models to Study Neuronal Apoptosis and Neurodegeneration *Frontiers in molecular neuroscience*.
- Guldvog, B. (2017). Nasjonalt screeningprogram mot tarmkreft; Status og behandling *Helsedirektoratet*.
- Halilovic, E., She, Q.B., Ye, Q., Pagliarini, R., Sellers, W.R., Solit, D.B., Rosen, N. (2010). - PIK3CA mutation uncouples tumor growth and cyclin D1 regulation from MEK/ERK and. *Cancer Res, 70*(17), 6804-6814.
- Hanahan, D., Weinberg, RA. (2011). - Hallmarks of cancer: the next generation. *Cell, 144*(5), 646-674.
- Hong, S., Kim, S., Kim, H.Y., Kang, M., Jang, H.H., Lee, W. . (2016). Targeting the PI3K signaling pathway in KRAS mutant colon cancer. . *Cancer Medicine, 5(2), 248–255.*
- Hotchkiss, R. S., Strasser, A., McDunn, J.E. (2009). Cell death. *The new England journal of medicine*.

- Jin, Z., El-Deiry, W.S. (2005). Overview of cell death signaling pathways. *Cancer biology and therapy*.
- Jourdain, A., Martinou, J.C. (2009). Mitochondrial outer-membrane permeabilization and remodelling in apoptosis. *Int j Biochem Cell Biol*.
- Kroemer, G., Galluzzi, L., Vandenabeele, P., Abrams, J., Alnemri, E., Baehrecke, E. (2009). Classification of cell death: recommendations of the Nomenclature Committee on Cell Death 2009. . *Cell Death and Differentiation, 16(1), 3–11.*
- Kwong, L. N., Dove, W.F. (2009). - APC and its modifiers in colon cancer. *Adv Exp Med Biol, 656*, 85-106.
- Larsen, I. K., Møller, B., Johannesen, T.B., Larønningen, S., Robsahm, T.E., Grimsrud, T.K., Ursin, G. (2016). Cancer incidence, mortality, survival and prevalence in Norway. *Cancer registry of Norway, Institute of population-based cancer research.*
- Lemmon, M. A., Schlessinger, J. (2010). - Cell signaling by receptor tyrosine kinases. *Cell, 141*(7), 1117-1134.
- Lievre, A., Bachet, J.B., Le-Corre, D., Boige, V., Landi, B., Emile, J.F., Cote, J.F., Tomasic, G., Penna, C., Ducreux, M., Rougier, P., Penault-Llorca, F., Laurent-Puig, P. (2006). - KRAS mutation status is predictive of response to cetuximab therapy in colorectal. *Cancer Res, 66*(8), 3992-3995.
- Logue, J. S., Morrison, D.K. (2012). - Complexity in the signaling network: insights from the use of targeted inhibitors. *Genes Dev, 26*(7), 641-650.
- Luo, F., Li, J., Wu, S., Wu, X., Chen, M., Zhong, X., Liu, K. . (2016). Comparative profiling between primary colorectal carcinomas and metastases identifies heterogeneity on drug resistance. . *Oncotarget, 7(39), 63937–63949.*
- Marsh, R., Samuel, J. (2007). Essentials of clinical oncology. *Jaypee brothers medical*.
- McCubrey, J. A., Steelman, L.S., Bertrand, F.E., Davis, N.M., Sokolosky, M., Abrams, S.L., Montalto, G., D'Assoro, A.B., Libra, M., Nicoletti, F., Maestro, R., Basecke, J., Rakus, D., Gizak, A., Demidenko, Z.N., Cocco, L., Martelli, A.M., Cervello, M. (2014). - GSK-3 as potential target for therapeutic intervention in cancer. *Oncotarget, 5*(10), 2881-2911.
- Mendoza, M. C., Er, E.E., Blenis, J. (2011). - The Ras-ERK and PI3K-mTOR pathways: cross-talk and compensation. *Trends Biochem Sci, 36*(6), 320-328.
- Navarro, M., Nicolas, A., Ferrandez, A., Lanas, A. (2017). - Colorectal cancer population screening programs worldwide in 2016: An update. *World J Gastroenterol, 23*(20), 3632-3642.
- Nejad, A. L., Yaghoobi, M.M. (2012). - Mutation Analysis of TP53 Tumor Suppressor Gene in Colorectal Cancer in Patients. *Iran J Basic Med Sci, 15*(1), 683-690.
- Ogino, S., Lochhead, P., Giovannucci, E., Meyerhardt, J.A., Fuchs, C.S., Chan, A.T. (2014). Discovery of Colorectal Cancer PIK3CA Mutation as Potential Predictive Biomarker: Power and Promise of Molecular Pathological Epidemiology. *Oncogene*.
- Ozono, E., Yamaoka, S., Ohtani, K. (2013). To Grow, Stop or Die? – Novel Tumor-Suppressive Mechanism Regulated by the Transcription Factor E2F. *Future Aspects of Tumor Suppressor Gene, Dr. Yue Cheng (Ed.), InTech, DOI: 10.5772/54510.*
- Pitts, T., Newton, TP., Bradshaw-Pierce, EL., Addison, R., Arcaroli, JJ., Klauck, PJ., Bagby, SM., Hyatt, SL., Purkey, A., Tentler, J.J., Tan, A.C., Messersmith, W.A., Eckhardt, S.G., Leong, S. (2014). - Dual pharmacological targeting of the MAP kinase and PI3K/mTOR pathway in preclinical models of colorectal cancer. *PLoS One, 9*(11), 0113037.
- Potter, D. S., Kelly, P., Denneny, O., Juvin, V., Stephens, L.R., Dive, C., Morrow, C.J. . (2014). BMX Acts Downstream of PI3K to Promote Colorectal Cancer Cell Survival

and Pathway Inhibition Sensitizes to the BH3 Mimetic ABT-737. . *Neoplasia (New York, N.Y.), 16(2), 147–157.*
- Promega. (2015). CellTox-Green Cytotoxicity Assay - Technical manual
- Promega. (2016). Caspase-Glo 3/7 Assay *Madison USA 2009*.
- Raynaud, F., Eccles, S., Clarke, PA., Hayes, A., Nutley, B., Alix, S., Henley, A., Di-Stefano, F., Ahmad, Z., Guillard, S., Bjerke, LM., Kelland, L., Valenti, M., Patterson, L., Gowan, S., Haven-Brandon, A., Hayakawa, M., Kaizawa, H., Koizumi, T., Ohishi, T., Patel, S., Saghir, N., Parker, P., Waterfield, M., Workman, P. (2007). - Pharmacologic characterization of a potent inhibitor of class I. *Cancer Res, 67*(12), 5840-5850.
- Reichert, J., Valge-Archer, VE. (2007). - Development trends for monoclonal antibody cancer therapeutics. *Nat Rev Drug Discov, 6*(5), 349-356.
- RIKEN. (2006). International Conference on System Biology. *Tokyo, Japan*.
- Roper, J., Sinnamon, MJ., Coffee, EM., Belmont, P., Keung, L., Georgeon-Richard, L., Wang, WV., Faber, AC., Yun, J., Yilmaz, OH., Bronson, RT., Martin, ES., Tsichlis, PN., Hung, KE. (2014). - Combination PI3K/MEK inhibition promotes tumor apoptosis and regression in PIK3CA. *Cancer Lett, 347*(2), 204-211.
- Samuels, Y., Waldman, T. . (2010). Oncogenic Mutations of PIK3CA in Human Cancers. . *Current Topics in Microbiology and Immunology, 347, 21–41.*
- Schell, M. J., Yang, M., Teer, J.K., Yin-Lo, F., Madan, A., Coppola, D., Monteiro, A.N.A., Nebozhyn, M.V., Yue, B., Loboda, A., Bien-Willner, G.A., Greenawalt, D.M., Yeatman, T.J. (2016). A multigene mutation classification of 468 colorectal cancers reveals a prognostic role for APC. *Nat Commun*.
- Shawver, L., Slamon, D., Ullrich, A. (2002). - Smart drugs: tyrosine kinase inhibitors in cancer therapy. *Cancer Cell, 1*(2), 117-123.
- She, Q., Solit, DB., Ye, Q., O' Reilly, KE., Lobo, J., Rosen, N. (2005). - The BAD protein integrates survival signaling by EGFR/MAPK and PI3K/Akt kinase. *Cancer Cell, 8*(4), 287-297.
- Szymański, P., Markowicz, M., Mikiciuk-Olasik, E. . (2012). Adaptation of High-Throughput Screening in Drug Discovery—Toxicological Screening Tests. *International Journal of Molecular Sciences, 13(1), 427–452.*
- Takayama, T., Miyanishi, K., Hayashi, T., Sato, Y., Niitsu, Y. (2006). Colorectal cancer: genetics of development and metastasis. *J Gastroenterol 41(3):185-92.*
- Tan, C., Du, X. (2012). KRAS mutation testing in metastatic colorectal cancer. *World J Gastroenterol.*
- Xiao-Lan, L., Jianbiao, Z., Zhi-Rong, C., Wee-Joo, C. (2015). p53 mutations in colorectal cancer- molecular pathogenesis and pharmacological reactivation. *World J Gastroenterol.*
- Ye, Q., Cai, W., Zheng, Y., Evers, BM., She, QB. (2014). - ERK and AKT signaling cooperate to translationally regulate survivin expression. *Oncogene, 33*(14), 1828-1839.
- Zhang, C., Zeng, X. (2013). Cell Proliferation in Drug Discovery and Development *Nova Science Publishers, Inc.*
- Zhao, B., Wang, L., Qiu, H., Zhang, M., Sun, L., Peng, P., Yuan, X. (2017). Mechanisms of resistance to anti-EGFR therapy in colorectal cancer. *Oncotarget, 8(3), 3980–4000.*

7. APPENDIX

APPENDIX 1: TRIS-LYSIS BUFFER

Stock solution of Lysis buffer I and Buffer II were prepared according to the tables below. The stock was stored at 4°C. Shortly before lyses of the cell pellet 919µl of lysis buffer stock I and II was supplemented with 1µl DTT (1M), 40µl 50xComplete (EDTA-free protease inhibitor cocktail, Roche, 1183617001), 20µl Phosphatase Inhibitor Cocktail 3 (Sigma, P004) and 20µl Phosphatase Inhibitor Cocktail 2 (Sigma, P5726), respectively.

BUFFER 1			
Buffer	Final concentration	Per ml Buffer	Stock (20ml)
1M Tris-HCl, pH 8,0	10mM	10µl	200µl
1M KCl	200mM	200µl	4ml
dH20		749µl	14,98ml

BUFFER 2			
Buffer	Final concentration	Per ml Buffer	Stock (20ml)
1M Tris-HCl, ph 8,0	10nM	10µl	200µl
1M KCl	200mM	200µl	4ml
0,5M EDTA	2mM	4µl	80µl
87% Glycerol	40%	460µl	9,2ml
10& NP-40	0,5%	50µl	1ml
dH20		276µl	5,52ml

APPENDIX 2: CELL MORPHOLOGICAL CHANGES (HCT116)

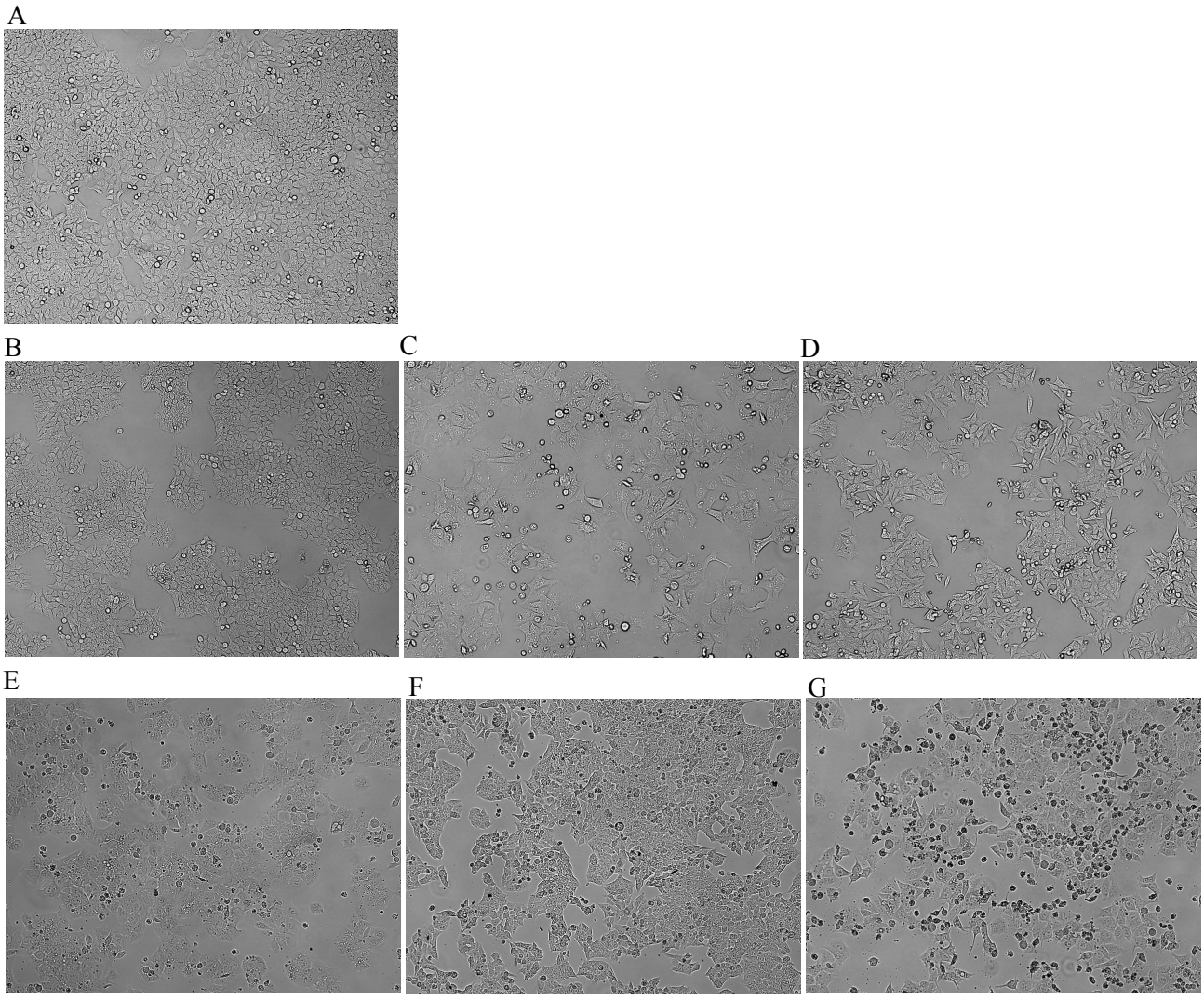

Figure 16: Microscopy images of HCT116 cells treated with inhibitors at a concentration of 10μM for 48h(10x). A: Untreated cells. B:PI:PI3K inhibitor. C:D1:p90RSK inhibitor. D: CT:GSK3 inhibitor. E: PI+D1:PI3K+p90RSK inhibitors. F: PI+CT:PI3K+GSK3 inhibitors. G: D1+CT:p90RSK+ GSK3 inhibitors.